

SiPM behavior at low temperatures

G.Collazuol
INFN Pisa

Overview

- Introduction
- Experimental methods
- Measurements and discussion
- Conclusions

Overview

Complete characterization of FBK SiPM in the temperature range $50\text{K} < T < 320\text{K}$

- 1) junction forward and reverse (breakdown) characteristics
- 2) gain, dark current, after-pulses, cross-talk
- 3) photon detection efficiency (PDE)

→ Improved SiPM performances at low temperature (w/ respect to T room):

- 1) lower dark noise by several orders of magnitude
- 2) after-pulsing probability constant down to $\sim 100\text{K}$ (then blow up)
- 3) PDE variations up to $\pm 50\%$ (depending on λ) down to $\sim 100\text{K}$
- 4) better timing resolution
- 5) better $V_{\text{breakdown}}$ stability against variations of T

→ SiPM is an excellent alternative to PMT at low T

...even more than at room temperature !!!

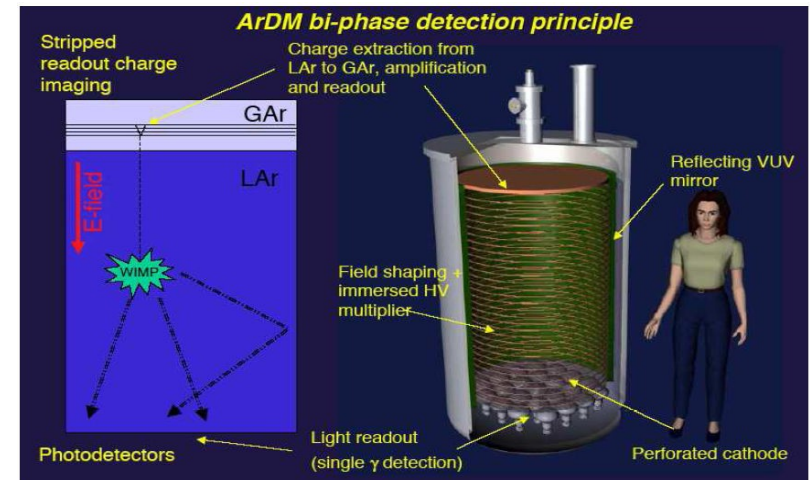
Applications w/ SiPM in cryogenic environments

Secondary scintillation from noble liquids generated by thick GEM (THGEM) for applications in neutrino physics, dark matter searches and PET

ArDM: Two-phase Ar detector using THGEM for DM search
[A.Rubbia et al., J. Phys. Conf. Ser. 39(2006)129]

!!! Need recording both ionization and scintillation with a threshold of $\leq 10\text{keV}$ (200 electrons)

A.Buzulutskov et al.
Vienna Conference VCI 2010 and
arXiv:1005.5216v1



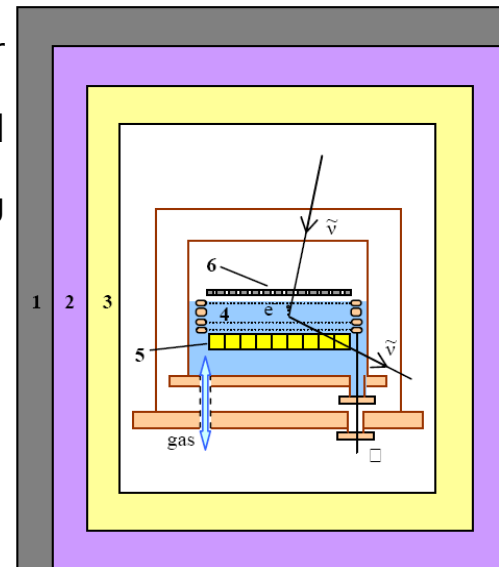
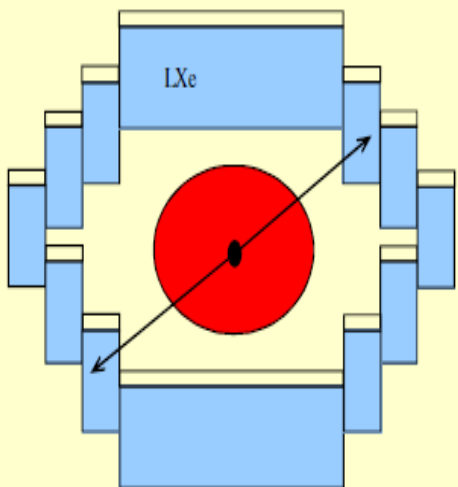
NIR emission spectrum of pure Ar (due to Ar I atomic lines) from avalanche scintillations at 750 Torr, gain ~ 30 , yield $\sim 1\text{ph/e}$. [M.M.Fraga et al. IEEE Trans.Nucl.Sci. 47(2000)933]

Two-phase Ar and Xe detectors using GEM/THGEM for coherent neutrino-nucleus scattering
[ITEP & Budker INP: Akimov et al. JINST 4 (2009) P06010]

!!! Need single electron counting

GEM-based two-phase Xe avalanche detector for PET:
3D liquid TPC recording 511 keV γ -rays
→ obtain superior ($\sim 1\text{mm}$) spatial resolution.
[Budker INP: CRDF grant RP1-2550 (2003)]

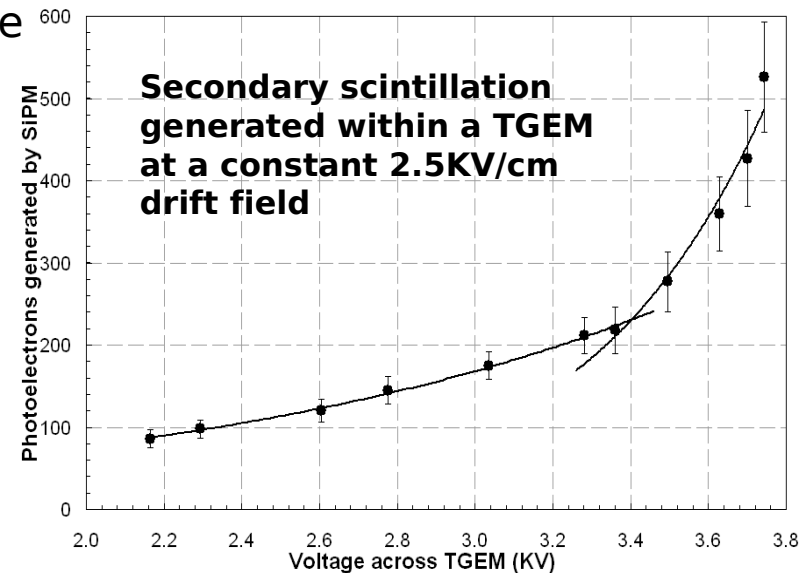
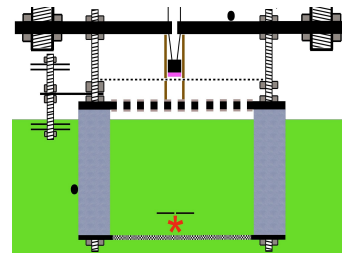
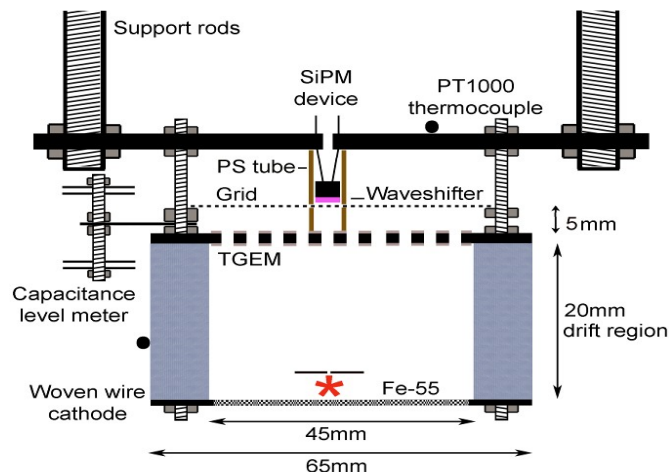
Need for Xe detector with 3D readout of both ionization and scintillation with a threshold of $> 100\text{ keV}$ (2000 electrons)



Applications w/ SiPM in cryogenic environments

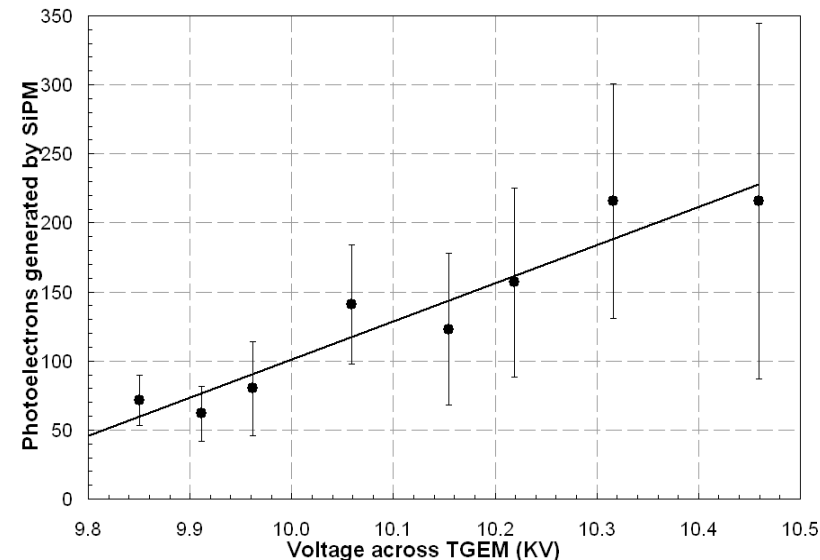
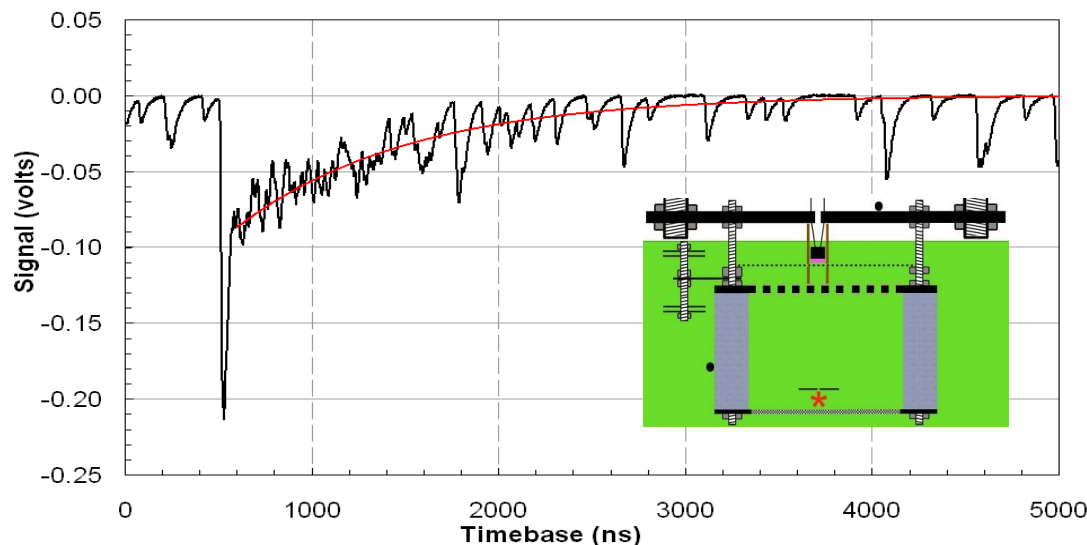
P.K.Lightfoot, et al.
J. Phys.: Conf. Ser. 179 (2009) 012014

Electroluminescence from the cold gas phase of a double phase Ar system



see talk by N.McConkey at this conference !!!

Electroluminescence from LAr



128nm VUV light produced within the TGM holes was then incident on an immersed SiPM device coated in the wavy shifter tetraphenyl butadiene (TPB), the emission spectrum peaked at 460nm in the high quantum efficiency region of the device

Vacuum vessel ($P < 10^{-3}$ mbar)

Experimental Setup

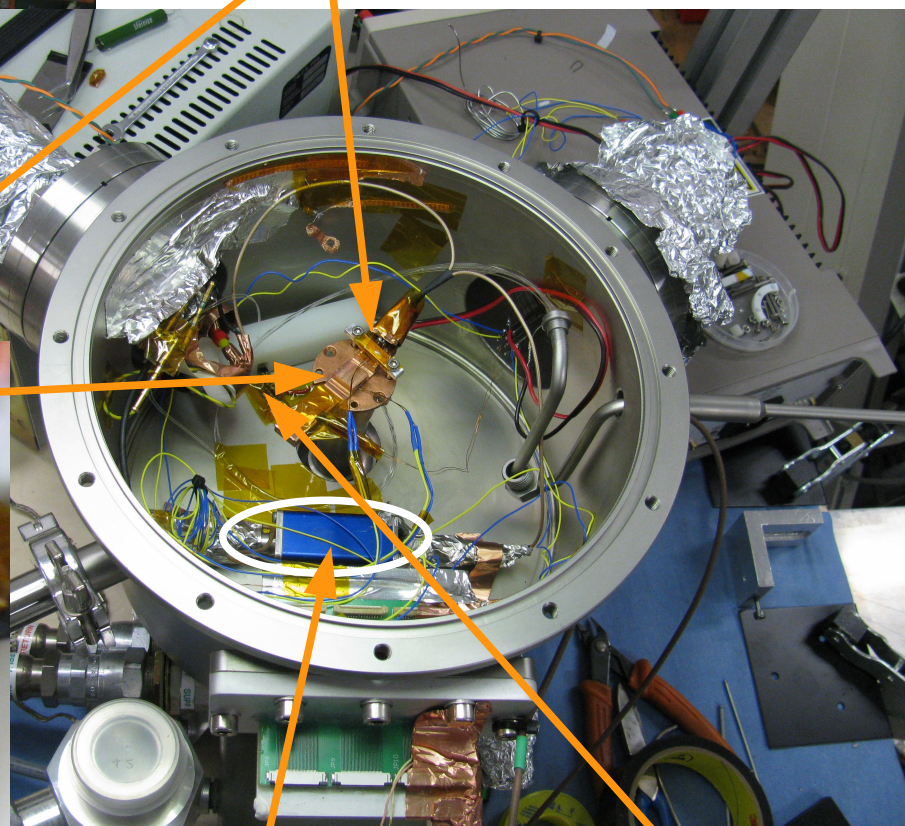
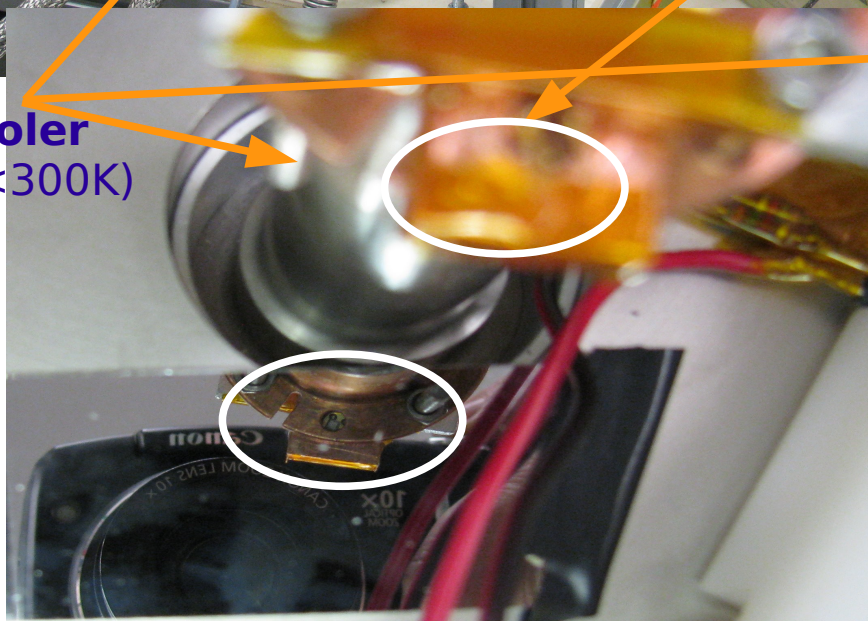


Halogen Lamp / Pulsed Laser

**Monocromator (200-900nm)
and neutral filters**

**Quartz fibers to
Calibrated Photodiode (outside)
and to SiPM (inside vessel)**

**Cryo-cooler
($50\text{K} < T < 300\text{K}$)**



Amplifier

**UV LED (380nm)
+ fibers to SiPM**

Experimental setup

Temperature control/measurement

- Close cycle, two stages, He cryo-cooler and heating with low R resistor
- Vacuum with $P < 10^{-3}$ mbar
- thermal contact (critical) with cryo-cooler head: SiPM within a copper rod + kapton (electrical insulation)
- T measurement with 3 pt100 probes
- Measurements on SiPM carried after thermalization, ie all probes at the same T
- check junction T with forward characteristic

Light sources

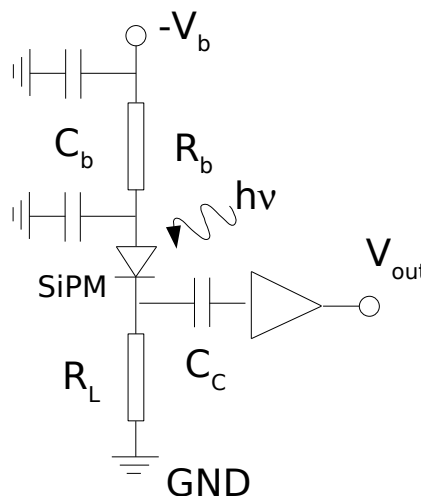
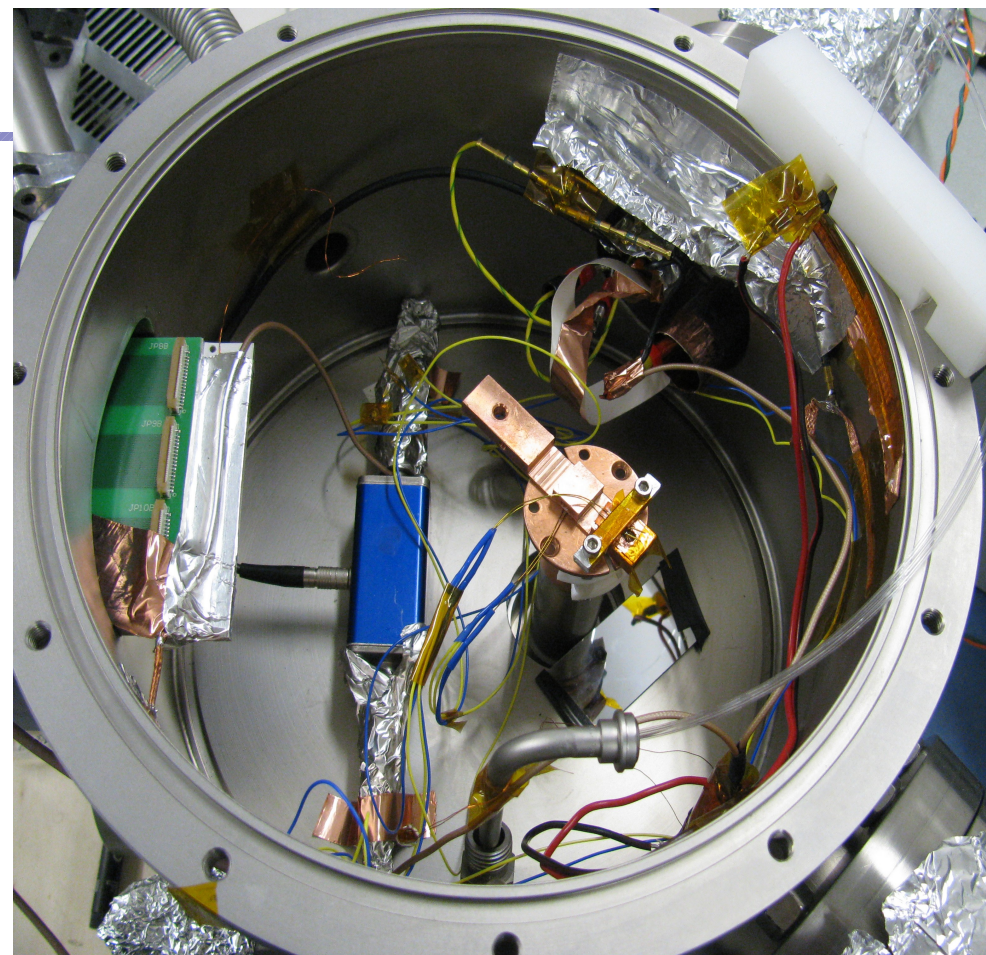
- CW: halogen lamp and UV LED ($\lambda \sim 380\text{nm}$)
- Pulsed: laser (30ps rms, $\lambda \sim 405\text{nm}$)

V_{bias} and current measurements

- Keytley 2148
Voltage/Current source/meter

Pulse/Wavef. measurements

- Care against HF noise
→ feedthroughs !!!
- Amplifier Photonique/CPTA
(gain ~ 30 , BW $\sim 300\text{MHz}$)
- Lecroy o.scope, 1GHz, 20GS/s



SiPM samples

FBK SiPM runII - 1mm^2
($V_{\text{br}} \sim 33\text{V}$, fill factor $\sim 20\%$)

- n-on-p shallow junction
- $4\mu\text{m}$ fully depleted region (active volume)
- no protective epoxy

SiPM equivalent circuit

Single cell model $\rightarrow (R_d || C_d) + (R_q || C_q)$

SiPM + load $\rightarrow (||Z_{\text{cell}}) || C_{\text{grid}} + Z_{\text{load}}$

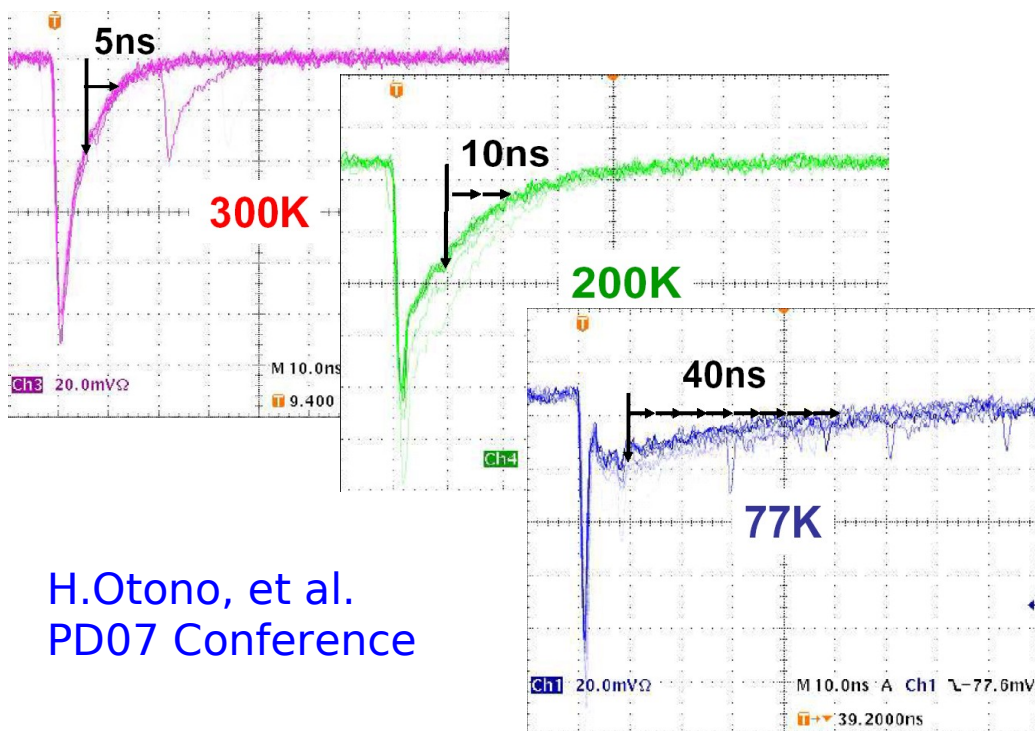
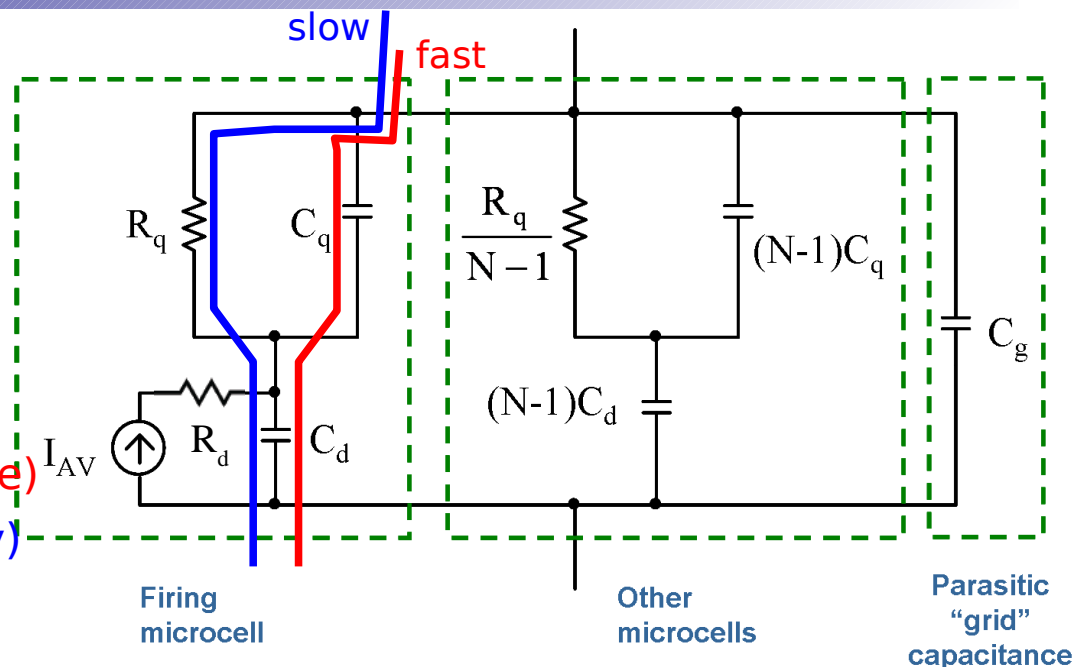
Signal = **slow** pulse (τ_d (rise), $\tau_{q\text{-slow}}$ (fall)) +
+ **fast** pulse (τ_d (rise), $\tau_{q\text{-fast}}$ (fall))

- τ_d (rise) $\sim R_d (C_q + C_d)$

- $\tau_{q\text{-fast}}$ (fall) = $R_{\text{load}} C_{\text{tot}}$ (fast; parasitic spike)

- $\tau_{q\text{-slow}}$ (fall) = $R_q (C_q + C_d)$ (slow; cell recovery)

F. Corsi, et al. NIMA 572(2007)



H.Otono, et al.
PD07 Conference

Pulse shape:

The two current components show different behavior with Temperature

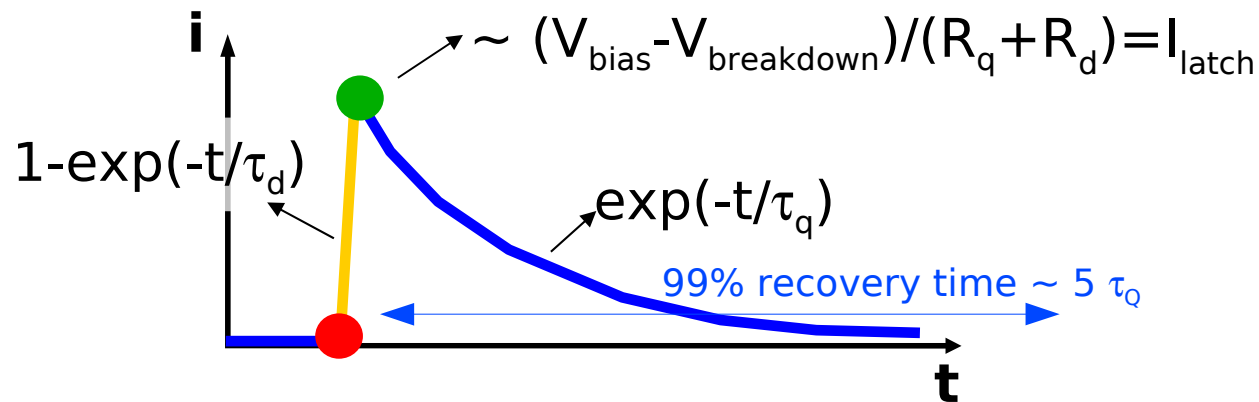
\rightarrow fast component is independent of T because stray C_q couple with external R_{load} (no dependence on T) while R_q is strongly dependent on T

(we used low light level, BW filters against noise and AC coupling \rightarrow difficult to disentangle the two components)

Gain and Recovery time

Fast Capacitor (cell) discharge and slow (+fast) recharge (roughly speaking)

If R_q is high enough the internal current decreases at a level such that statistical fluctuations may quench the avalanche



$$\Delta V \equiv (V_{\text{bias}} - V_{\text{Breakdown}})$$

overvoltage

The leading edge of the signal is much faster than trailing edge:

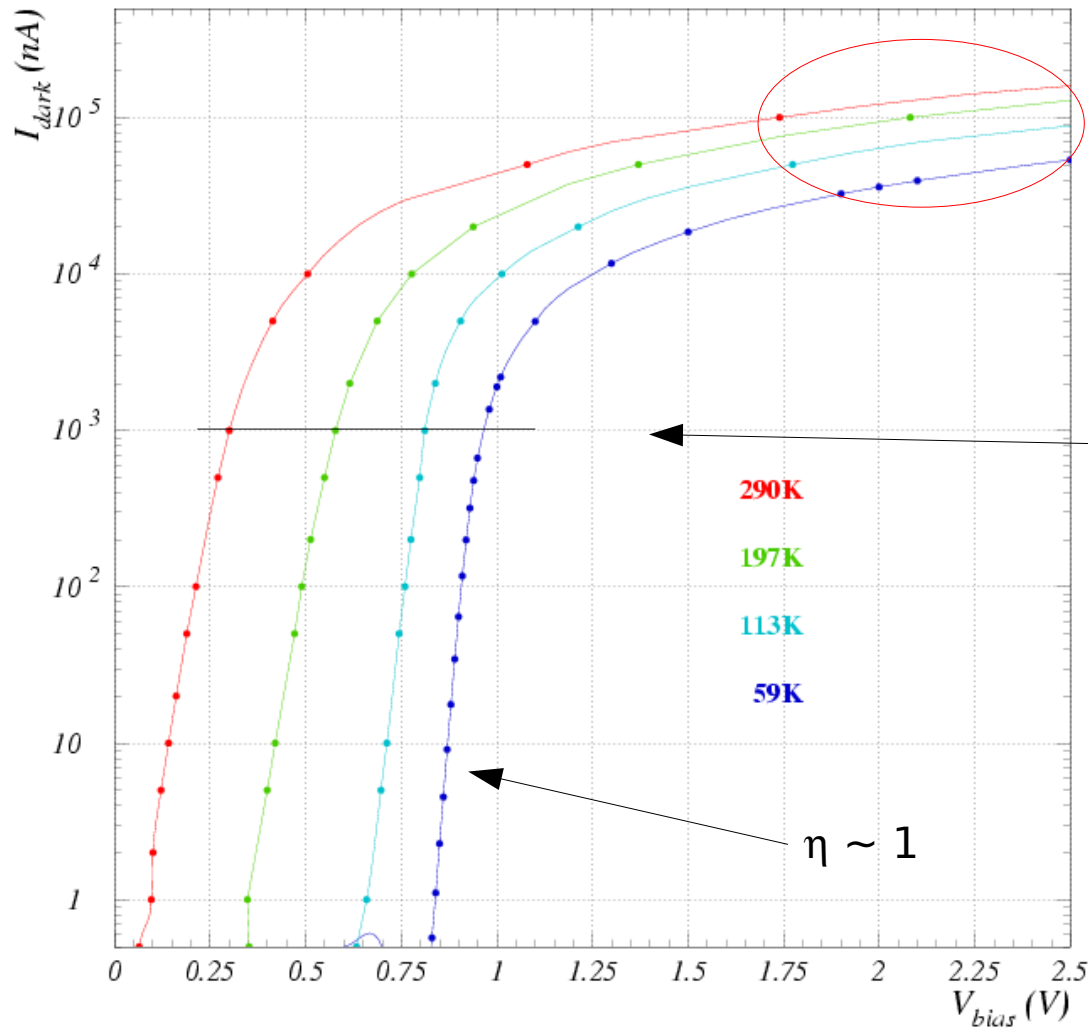
1. $\tau_d = R_d C_d \ll R_q C_q = \tau_q$
2. turn-off mean time is very short (if R_q is sufficiently high, $I_{\text{latch}} \sim 10 \mu\text{A}$)

Recovery time:

increases at low T due to polysilicon R_q while C_d is independent of T

Gain $\sim C_d \Delta V \rightarrow$ independent of T
at fixed Over-Voltage (ΔV)

I-V measurements: forward bias



③ **Ohmic** behavior at high current

Linear fit $\rightarrow R_{series} \sim R_q / N_{cells}$

② **Voltage drop** (V_d) decreases linearly with T decreasing (e.g. at $1\mu A$)

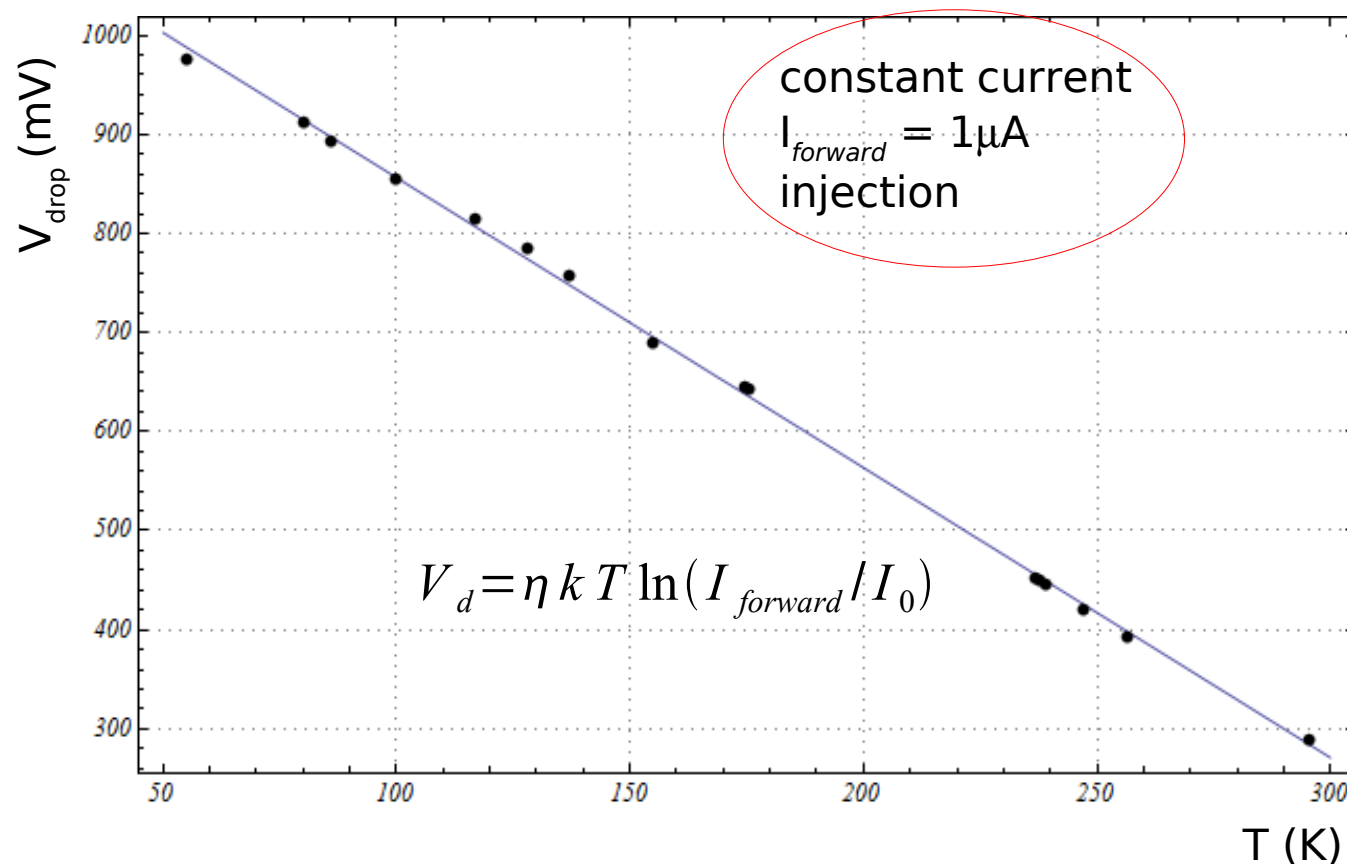
① **Forward current** $J_F \sim \exp(V_d \frac{q}{\eta k T})$

Diffusion dominating: $\eta \rightarrow 1$

Recombination dominating: $\eta \rightarrow 2$

I-V measurements: forward bias

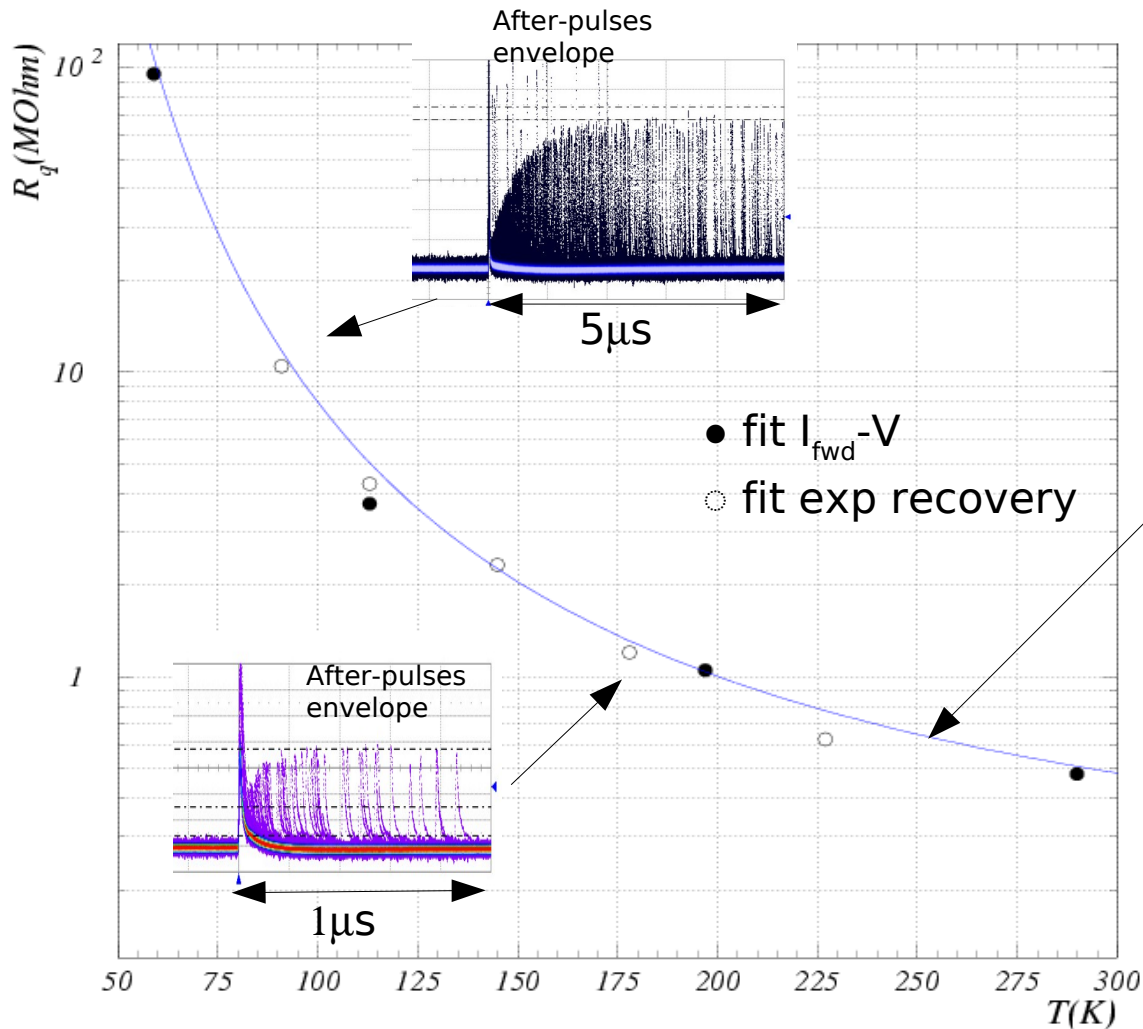
Voltage drop at fixed forward current → precise **measurement of junction T**



- linear dependence with slope $dV_{\text{drop}}/dT|_{1\mu\text{A}} \sim 3\text{mV/K}$
- **precise calibration/probe of junction Temperature**

Series Resistance vs T

- 1) Fit at high V of forward characteristic → **measurement of series resistance R_s**
- 2) Exponential recovery time (afterpulses envelope) → **measurement of R_s**

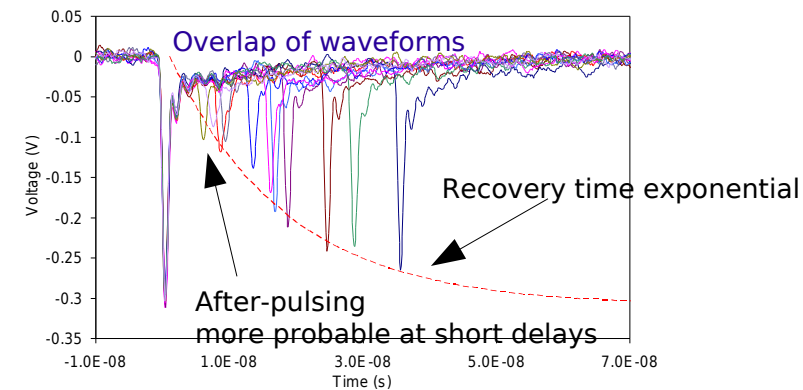


Measurements (1) and (2) consistent
 → **dominant effect from quenching resistor R_q**
 (gives R bulk smaller effect)

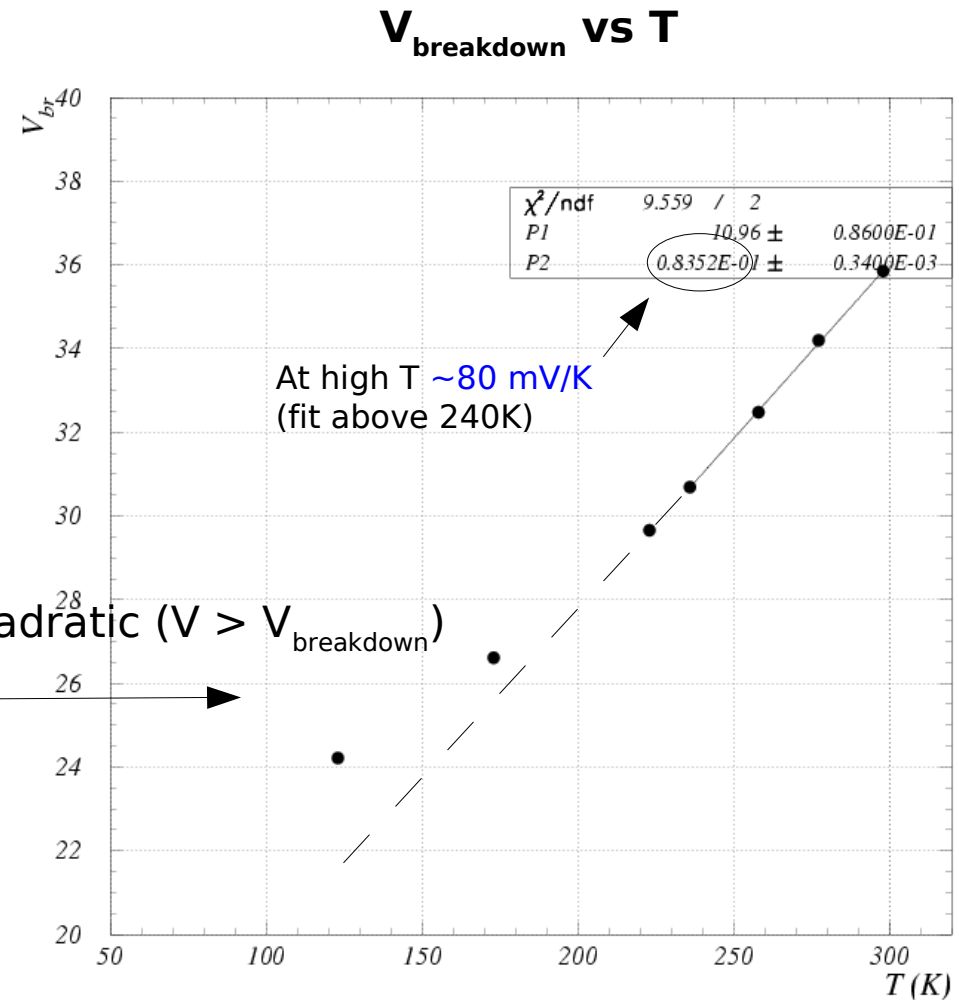
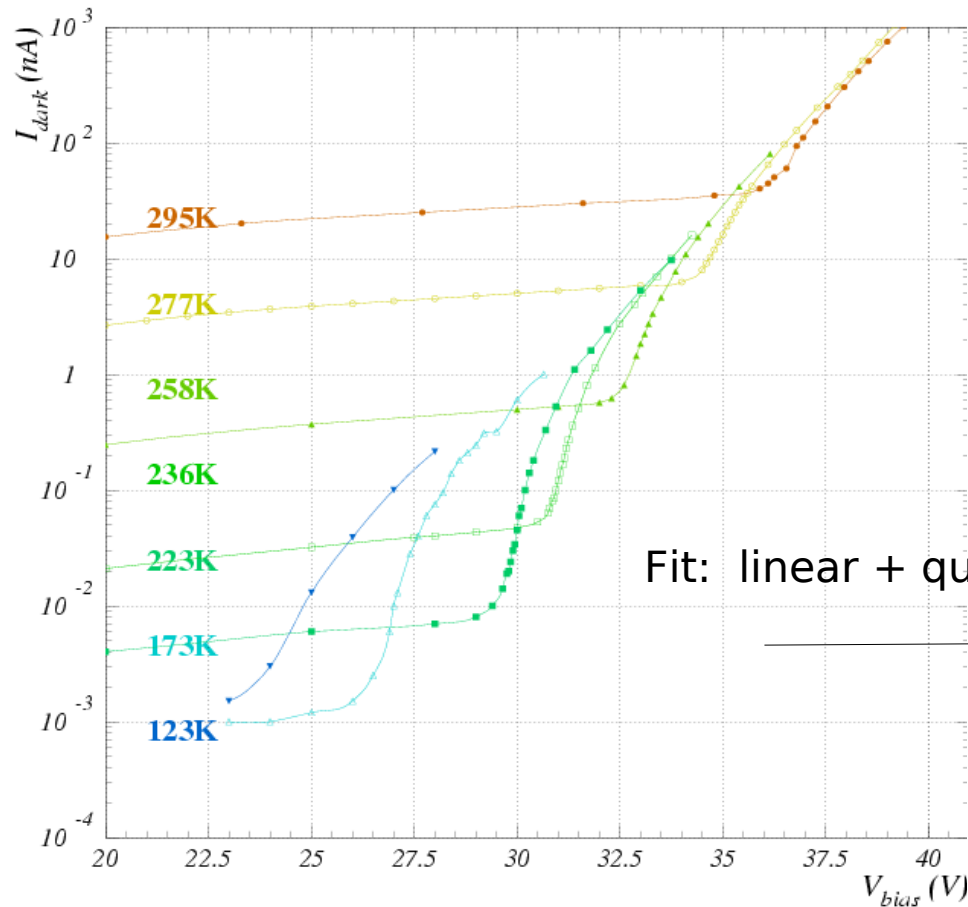
Empirical fit:

$$R_q(T) \sim 0.13 (1 + 300/T e^{300/T}) M\Omega$$

Afterpulses envelope



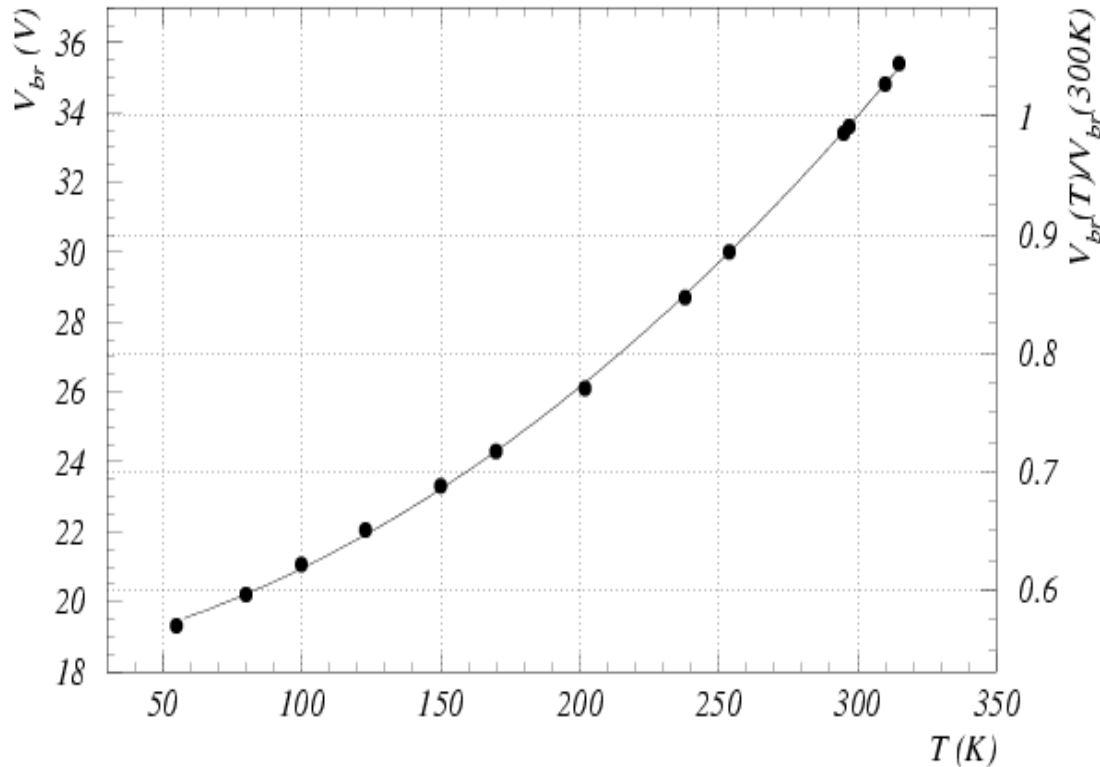
I-V measurements: reverse bias



Avalanche breakdown voltage decreases due to larger carriers mobility at low T \rightarrow **larger ionization rate** (at constant electric E field)

V breakdown vs T

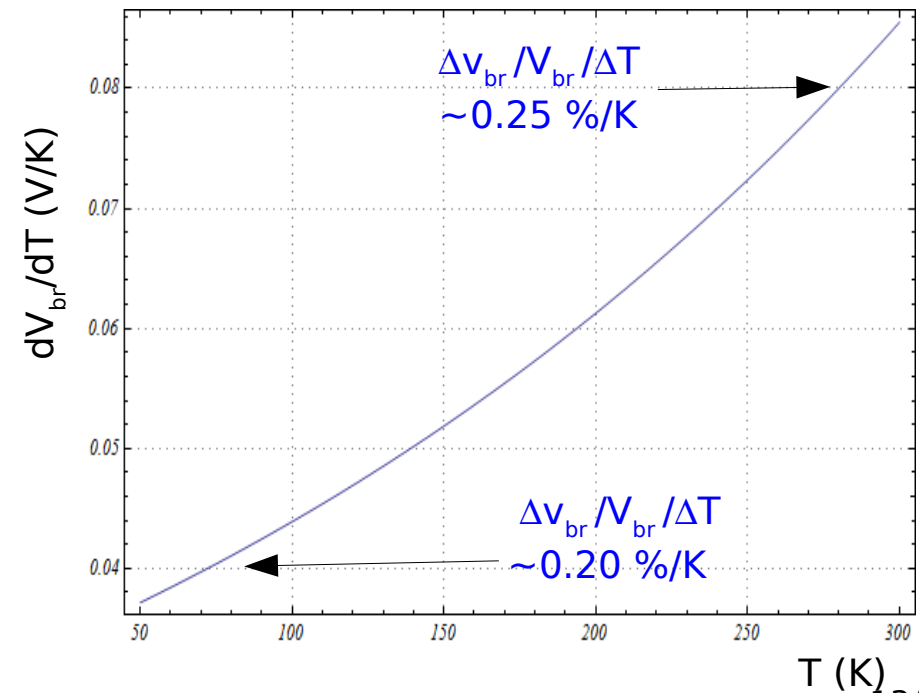
Breakdown Voltage



Consistent with Baraff model for abrupt junctions with doping $\sim 5 \cdot 10^{13} \text{ cm}^{-3}$

slightly better stability at low T

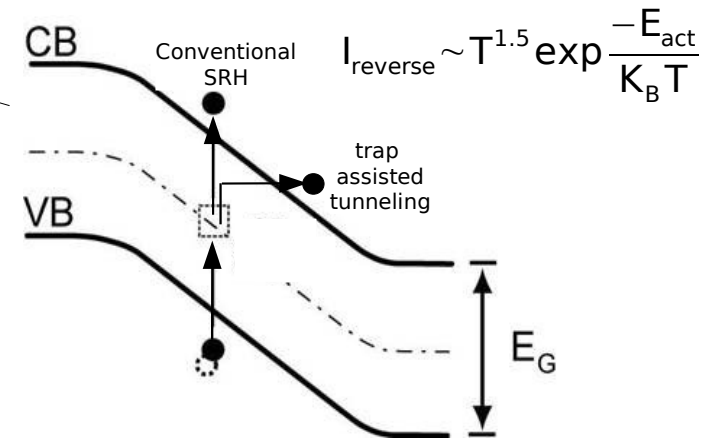
Temperature coefficient



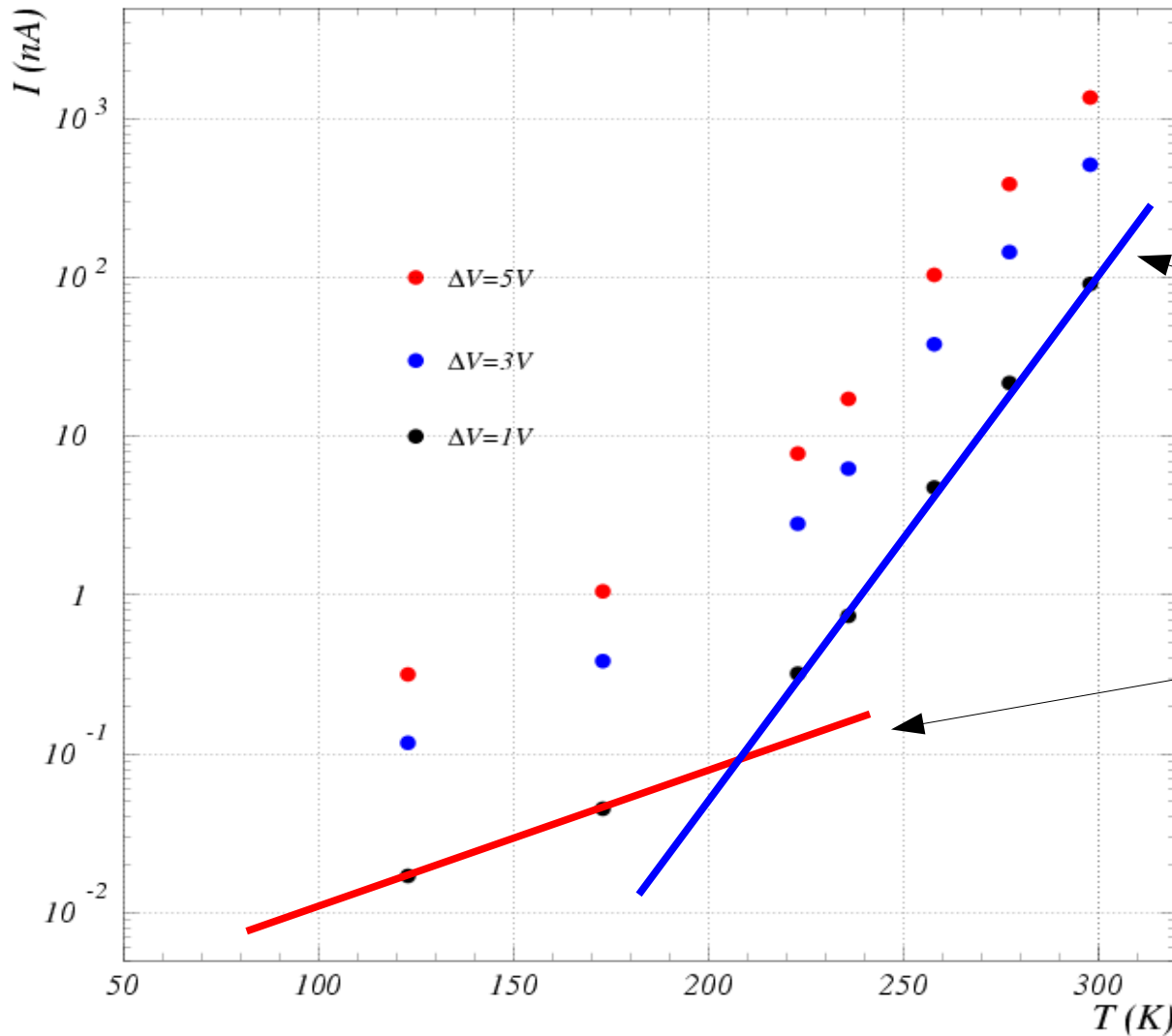
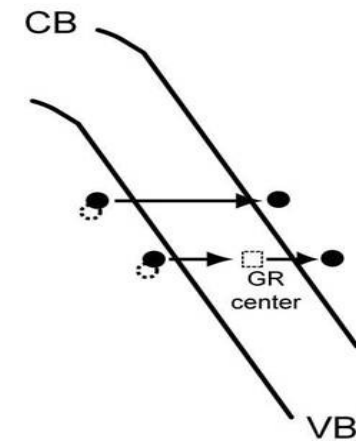
Dark current vs T (constant ΔV)

Main noise mechanisms
(minority carriers diffusion noise negligible):

1) **Generation/Recombination SRH noise** (enhanced by trap assisted tunneling)

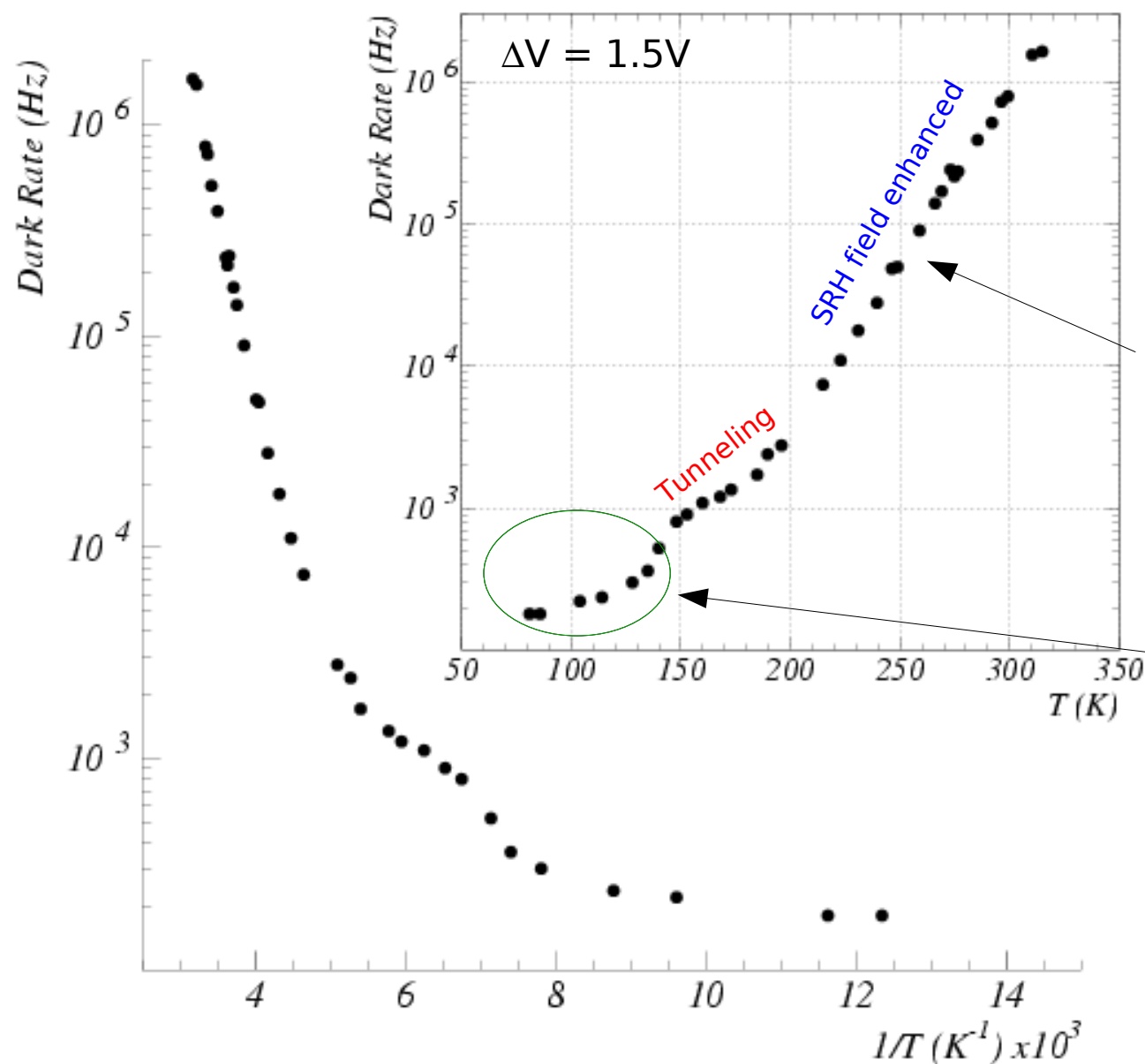


2) **Band-to-band Tunneling noise** (strong dependence on the Electric field profile)



Tunnel noise dominating
for $T < 200K$ (FBK devices)

Dark count rate vs T (constant ΔV)



Measurement of **counting rate of ≥ 1 p.e.** at fixed $\Delta V = 1.5V$ (\rightarrow constant gain)

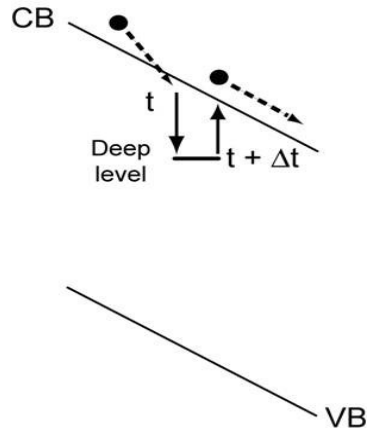
$$DCR \sim T^{1.5} \exp \frac{-E_{act}}{K_B T}$$

Activation energy $E_{act} \sim 0.36eV$

??? onset of carriers freeze-out (carrier losses at very low T due to ionized impurities acting as shallow traps)
Under investigation

After-Pulsing (AP)

Carrier trapping and delayed release



$$P_{\text{afterpulsing}}(t) = P_c \cdot \frac{\exp(-t/\tau)}{\tau} \cdot P_{\text{trigg}} \propto \Delta V^2 \quad \sim \text{Few \% level at 300K}$$

avalanche triggering probability
 $\propto \Delta V(t)$

τ : trap lifetime
 depends on trap level position

quadratic dependence on ΔV

P_c : trap capture probability

\propto carrier flux (current) during avalanche $\propto \Delta V$

$\propto N$ traps

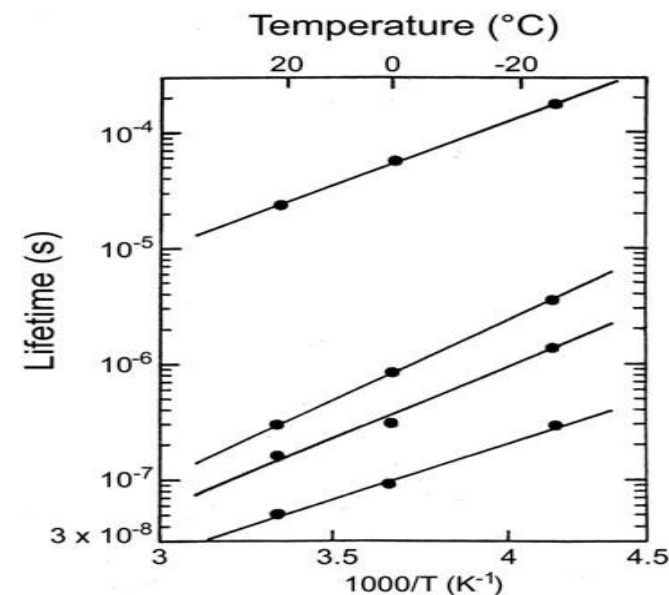
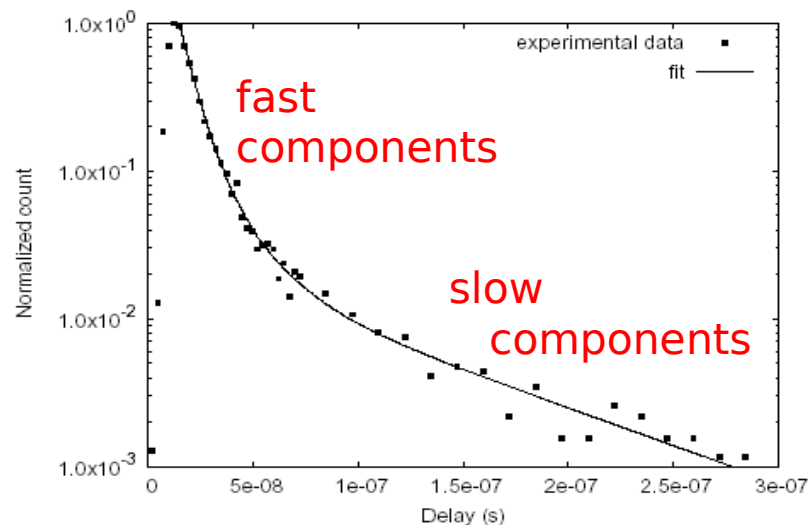


Fig. 10. Spectrum of the delay time from the primary pulse to the after-pulse.

S.Cova, A.Lacaita,
 G.Ripamonti, IEEE EDL (1991)

After-Pulses vs T (constant ΔV)

Measurement by waveform analysis:

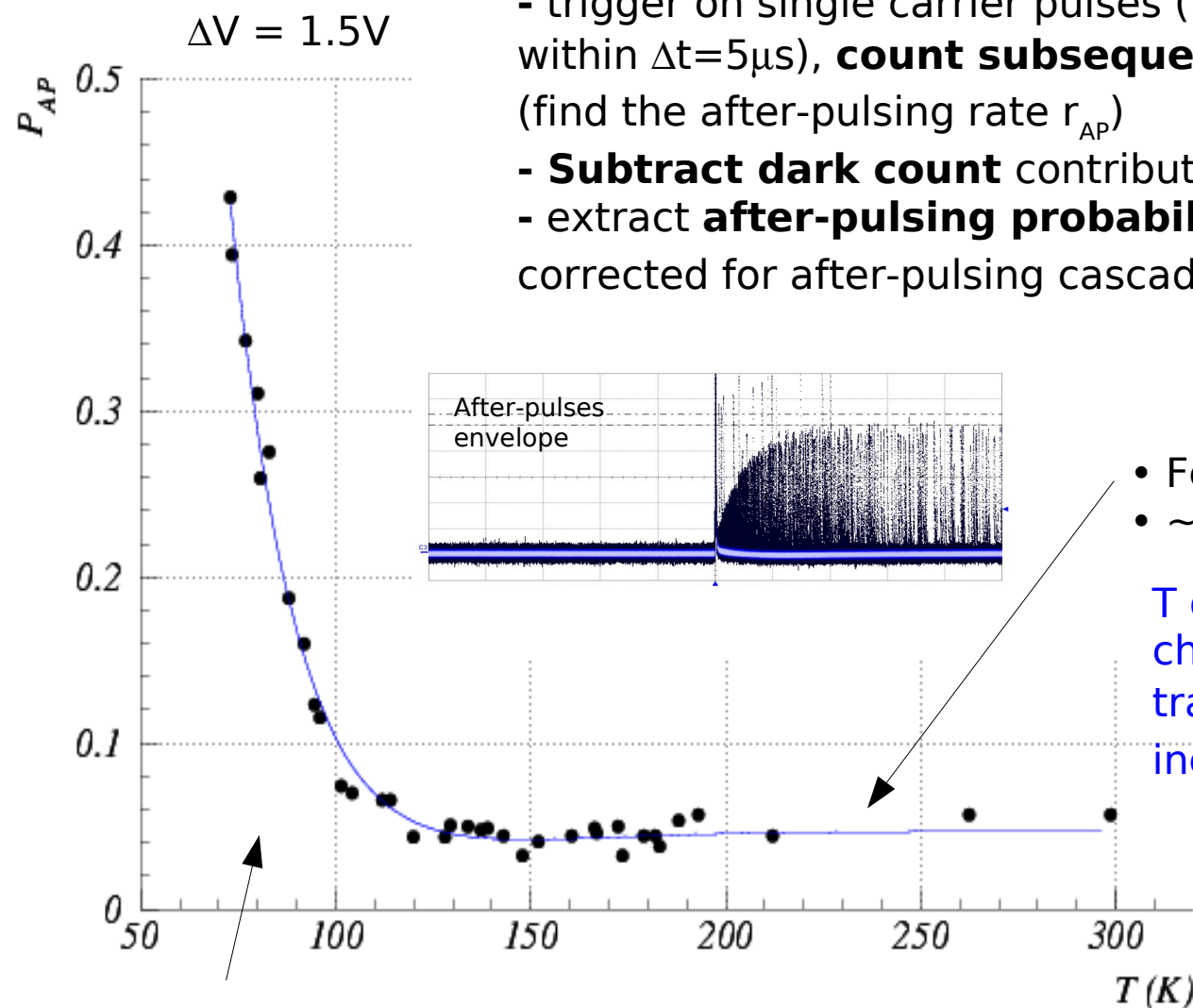
- trigger on single carrier pulses (with no preceding pulses within $\Delta t = 5\mu s$), **count subsequent pulses** within $\Delta t = 5\mu s$ (find the after-pulsing rate r_{AP})

- **Subtract dark count** contribution

- extract **after-pulsing probability** P_{AP}

corrected for after-pulsing cascade

$$P_{AP} = \frac{r_{AP}}{1 + r_{AP}}$$



- Few % at room T
- ~constant down to ~120K

T decreasing: increase of characteristic time constants of traps (τ_{traps}) is compensated by increasing cell recovery time (R_q)

- several % below 100K

T < 100K: new trapping centers active possibly related to carrier freeze-out (under investigation)

→ On-going work:
analysis of life-time evolution vs T
of the various traps (at least 3 found)

DR, AP, Gain, X-talk vs ΔV (constant T)

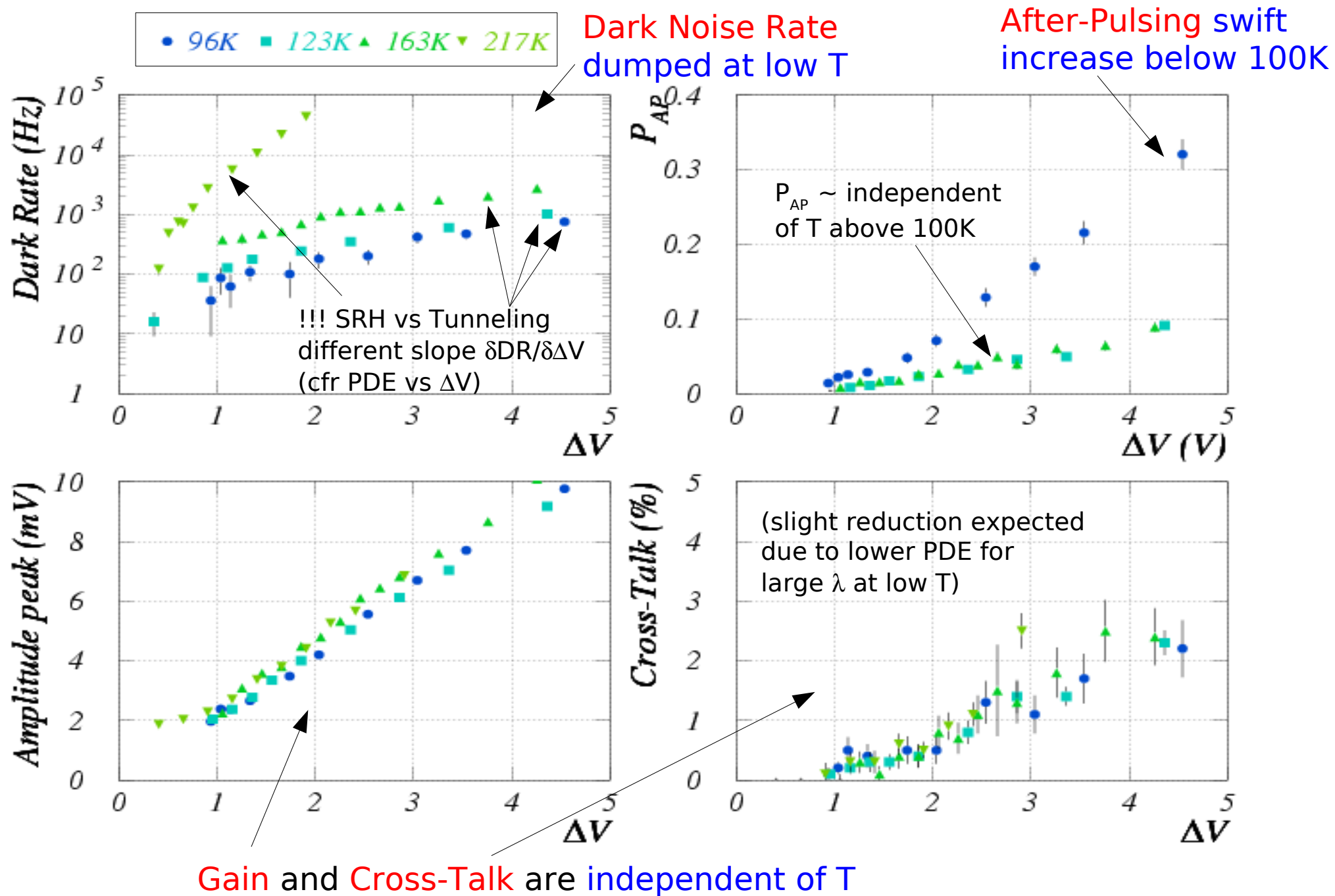
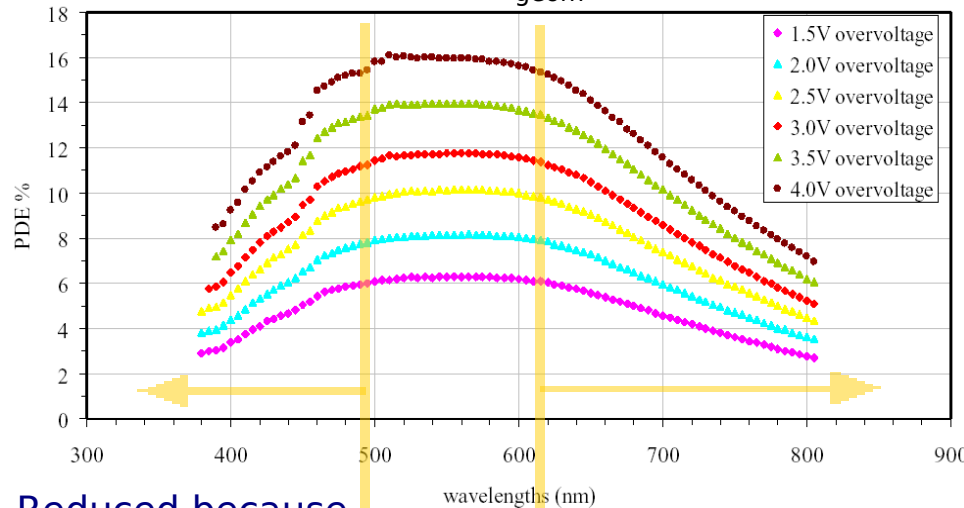


Photo-Detection Efficiency (PDE) vs ΔV and λ

SiPM with $\epsilon_{\text{geom}} \sim 22\%$



Reduced because avalanche triggered by holes (and ARC)

Reduced because low QE

PDE dependence on λ (at different ΔV) - room T

PDE =

ϵ_{geom} (fraction of active area)

X

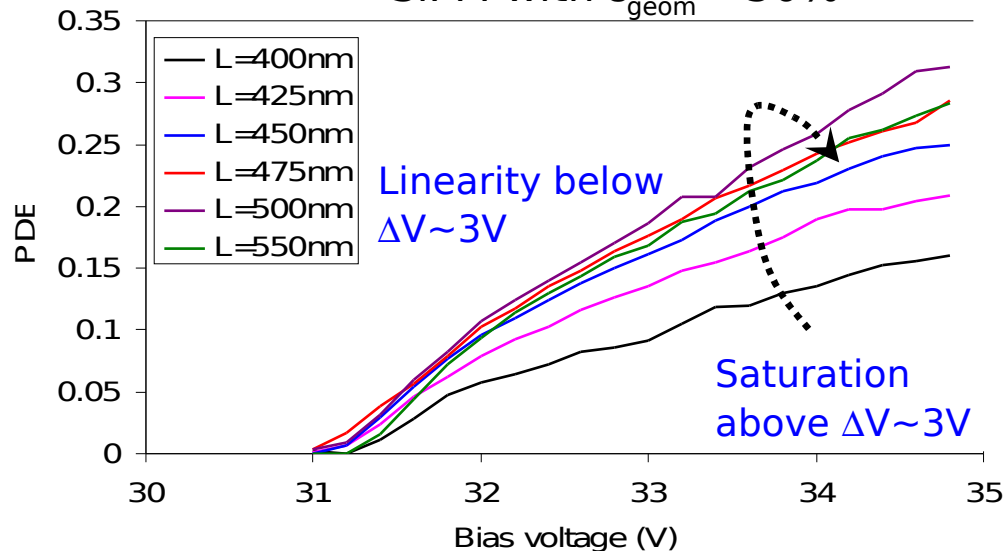
QE (efficiency of photo-conversion)

X

P_{trigg} (avalanche triggering probability)

Expected to be T dependent

SiPM with $\epsilon_{\text{geom}} \sim 50\%$



Linearity below $\Delta V \sim 3V$

Saturation above $\Delta V \sim 3V$

PDE dependence on ΔV (at different λ) - room T

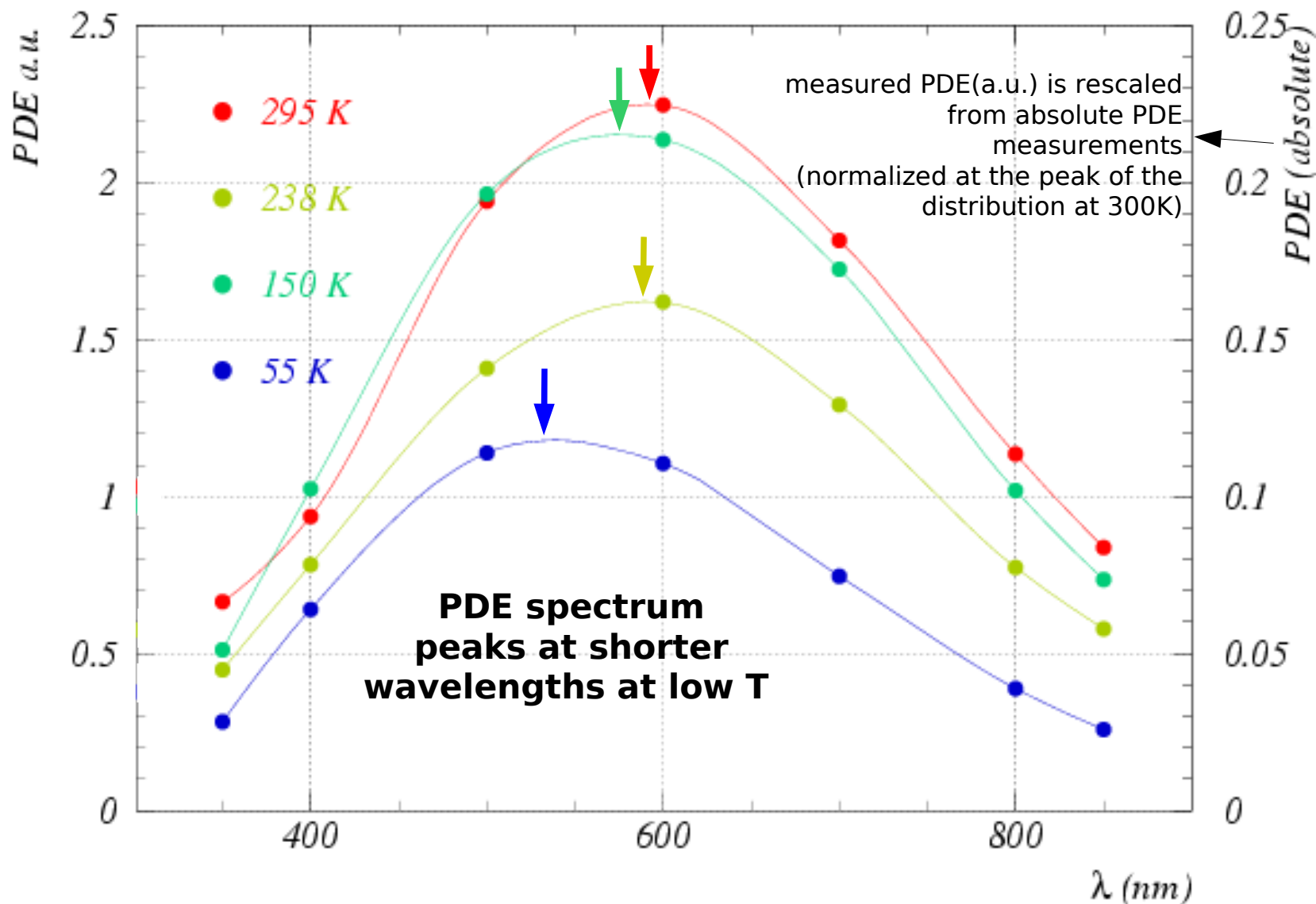
PDE vs λ (constant $\Delta V=2V$) - halogen lamp (CW)

Measure \rightarrow

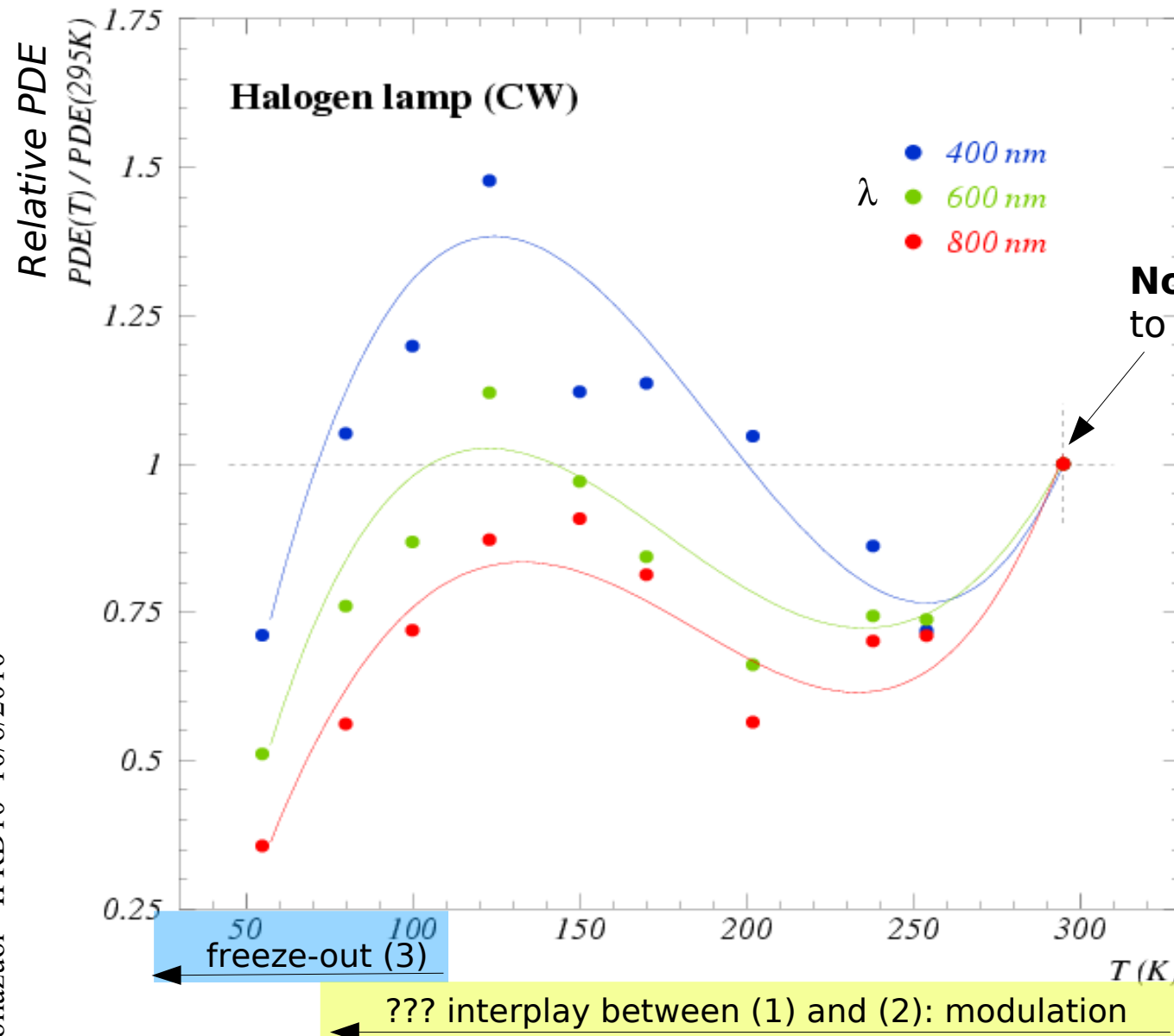
- I_{siPM} / G = current drawn by SiPM / SiPM gain
- I_{photons} = rate of photons by calibrated photo-diode

\rightarrow Find: $PDE = I_{\text{siPM}} / G / I_{\text{photons}}$

which differs from absolute PDE but for a common factor due to different photon acceptance of SiPM wrt calibrated diode (different light paths)



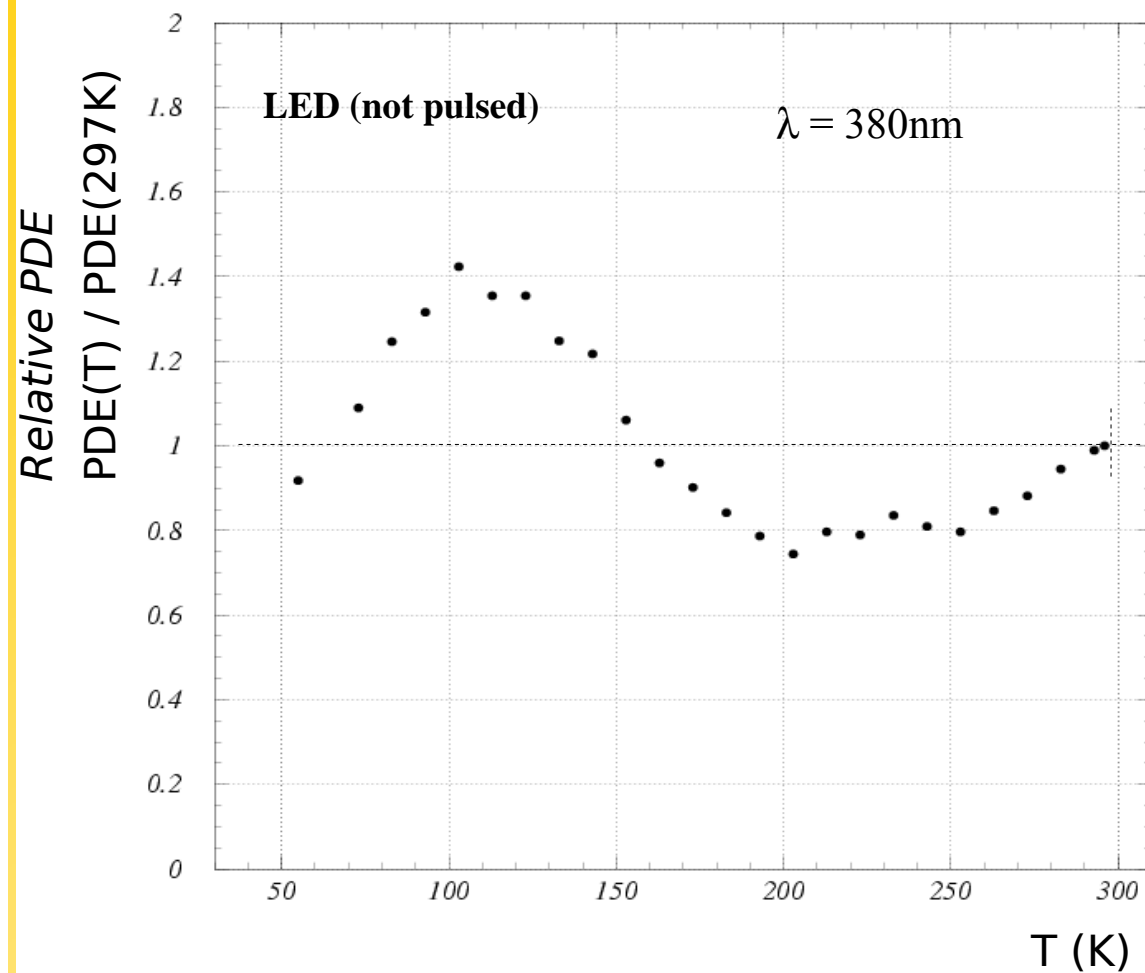
PDE vs T (constant $\Delta V=2V$) - halogen lamp (CW)



$$PDE = I_{sipa} / G / I_{photons}$$

PDE vs T ($\Delta V=2V$) - LED and Laser

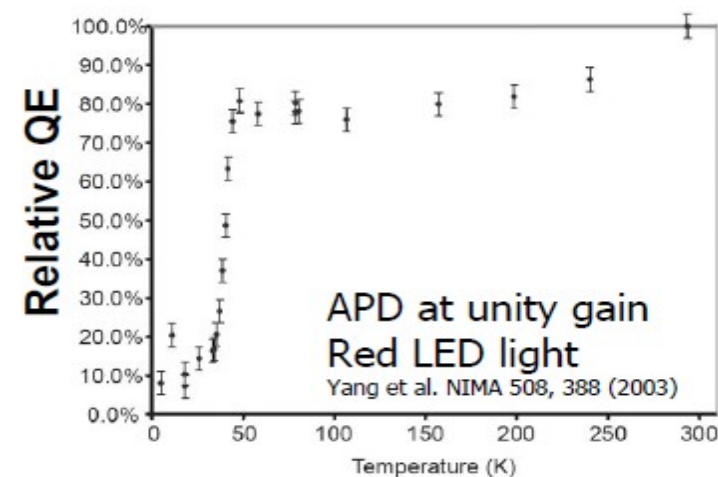
PDE dependence on T at constant gain:
similar results with LED (cont. light - 380nm)
and Laser (pulsed light - 405nm)



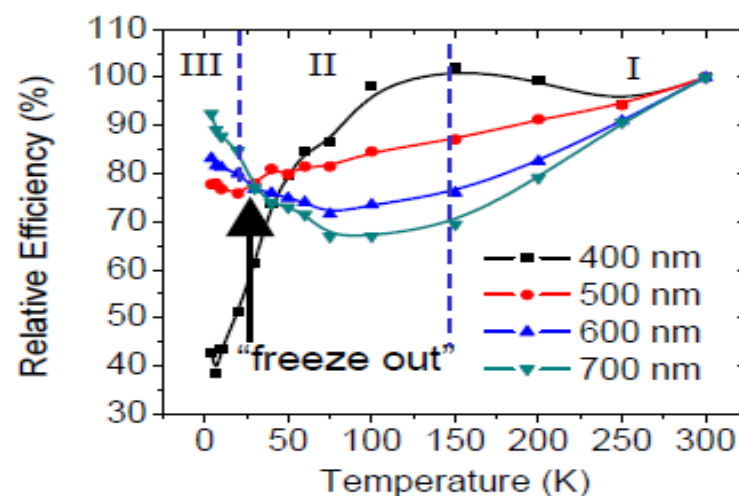
$$PDE(T) \equiv I_{SiPM}(T) / I_{LED}$$

Normalization with PDE at T=297K

Some common features
with APDs (proportional mode)



APD at $400\text{nm} < \lambda < 700\text{nm}$
Johnson et al, IEEE NSS 2009

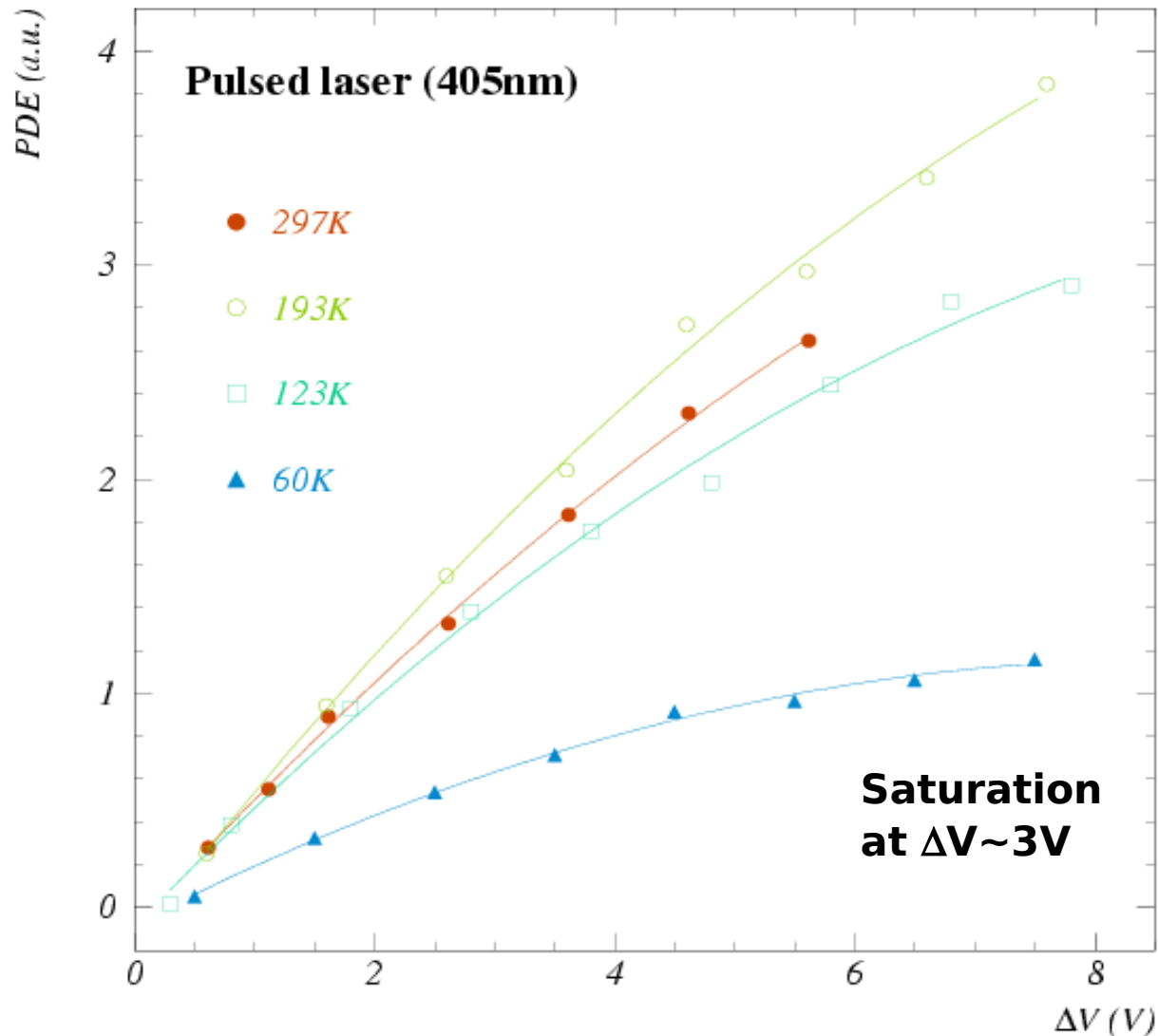


Additional effects in APD
(depletion region depends on T, ...)

PDE vs ΔV (constant T) – pulsed laser (405nm)

Measure →

- I_{pe} = average number of photo-el. in coincidence with laser trigger x trigger rate
- $I_{photons}$ = average rate of photons measured by calibrated photo-diode



→ Find: $PDE = I_{pe} / I_{photons}$

which differs from absolute PDE but for a common factor due to different photon acceptance of SiPM wrt calibrated diode (different light paths)

Understanding PDE vs T: 1D model

Preliminary results

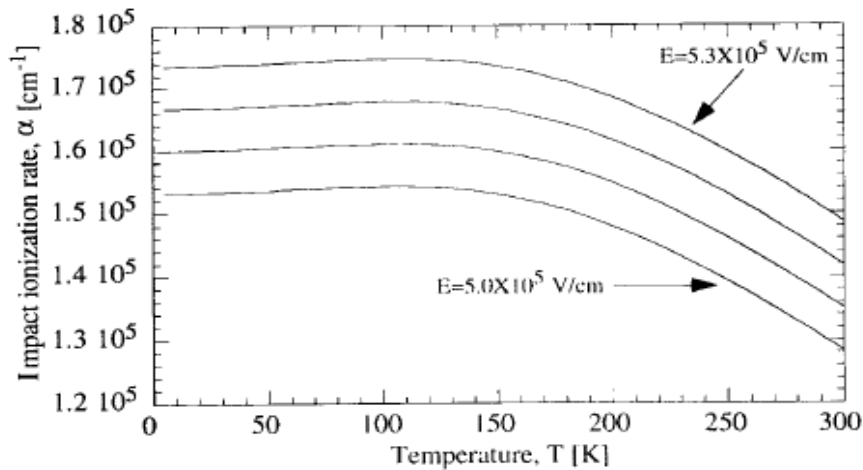
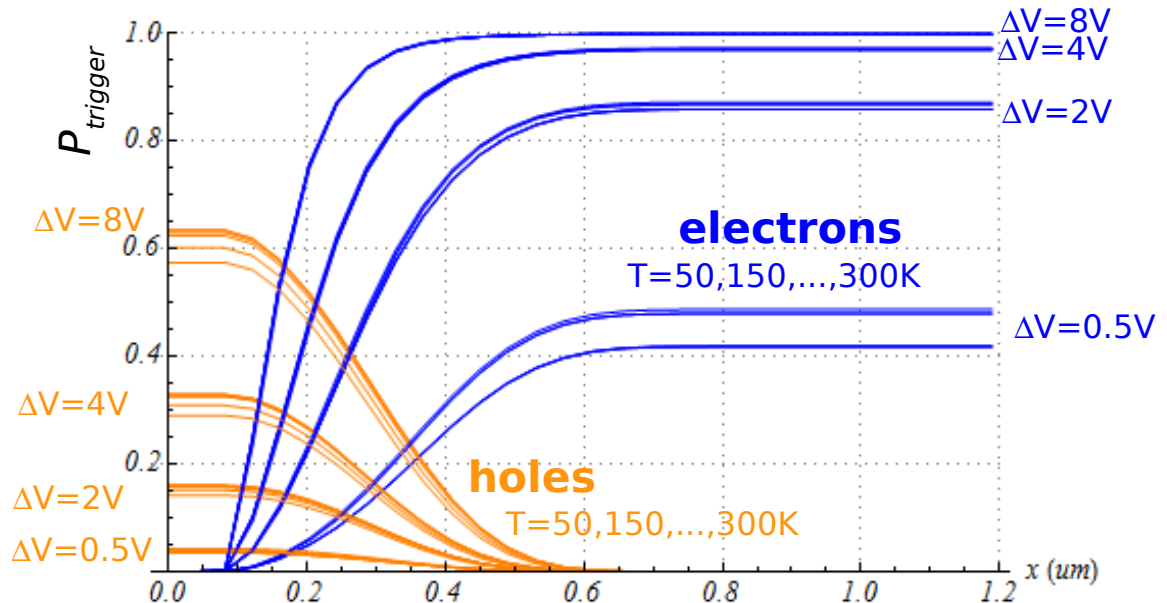
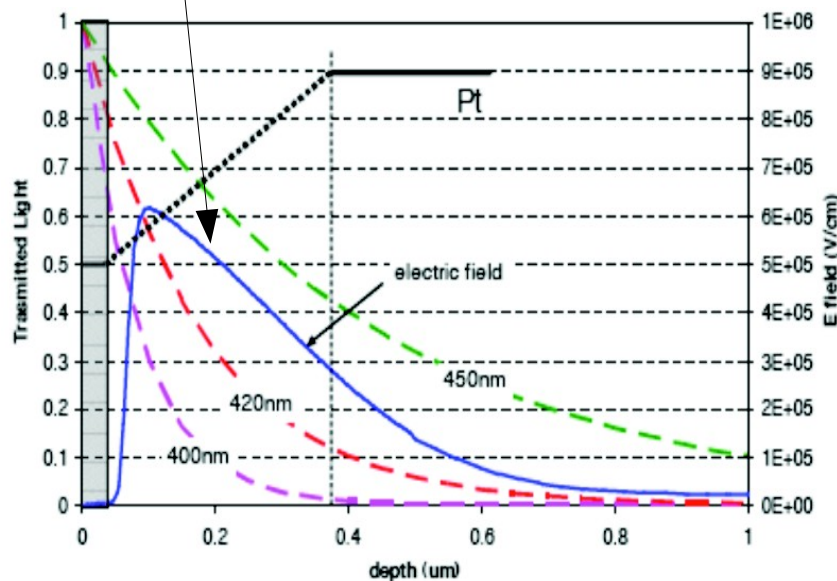


FIGURE 1.43. The impact ionization rate α as a function of temperature T_A with the electric field E as a parameter calculated from Okuto and Crowell's (85) model.

Breakdown voltage

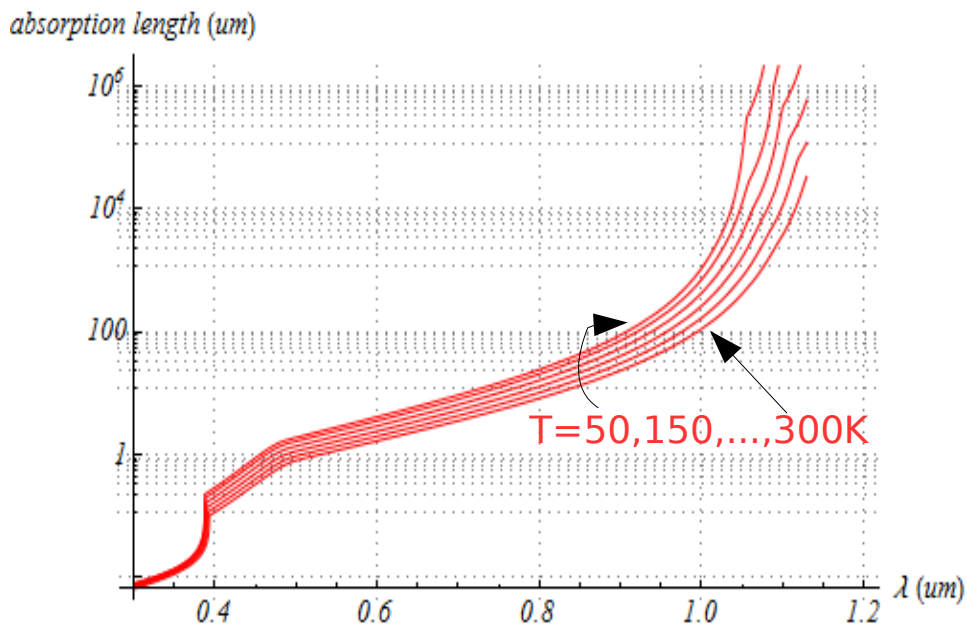
Avalanche triggering probability for electrons and holes ($P_{\text{trigger}e}$, $P_{\text{trigger}h}$) (using differential equations method after Oldham et al, IEEE TNS 19 (1972) 1056)

**E field profile +
+ impact ionization**



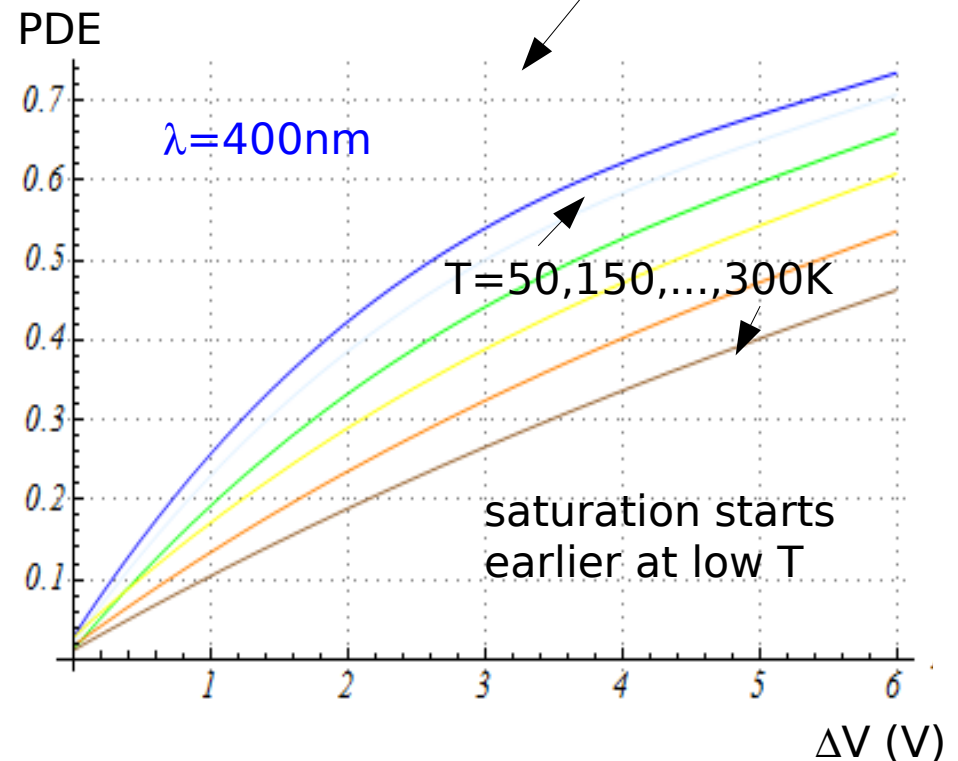
Understanding PDE vs T: 1D model

avalanche triggering probability +
+ light absorption length in Si ($1/\alpha$)

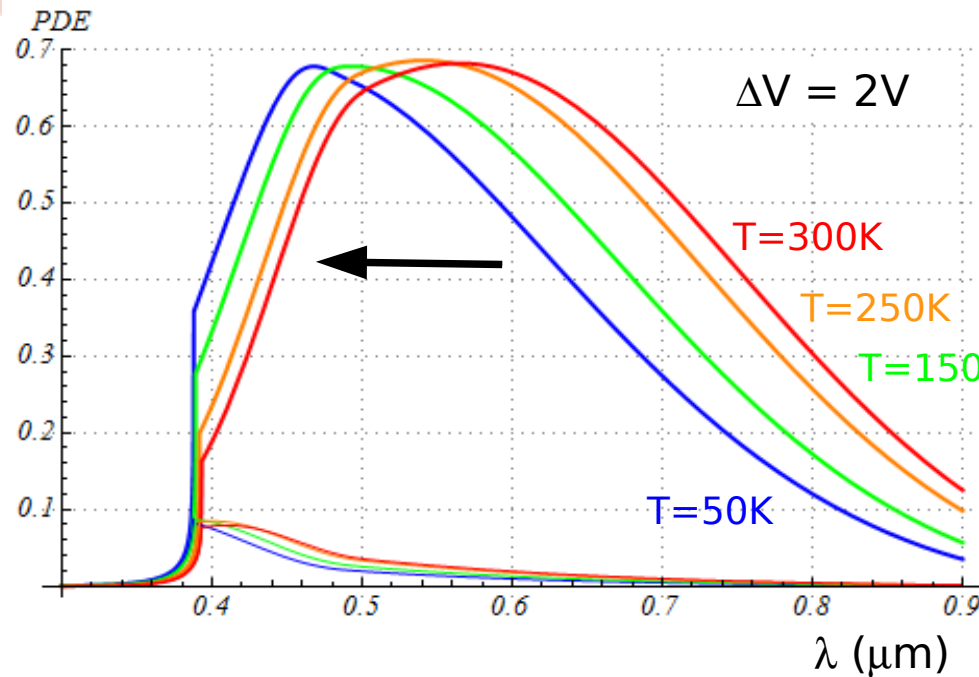


Rajkanan et al, Solid State Ele 22 (1979) 793
Accounting E_{gap} variations with T, etc...

PDE as a function of ($\lambda, T, \Delta V$)
obtained by the convolution of
 $P_{\text{trigg}}(x)$ and $\alpha \exp(-\alpha x)$
(integrated over the depletion layer)



Understanding PDE vs T: 1D model

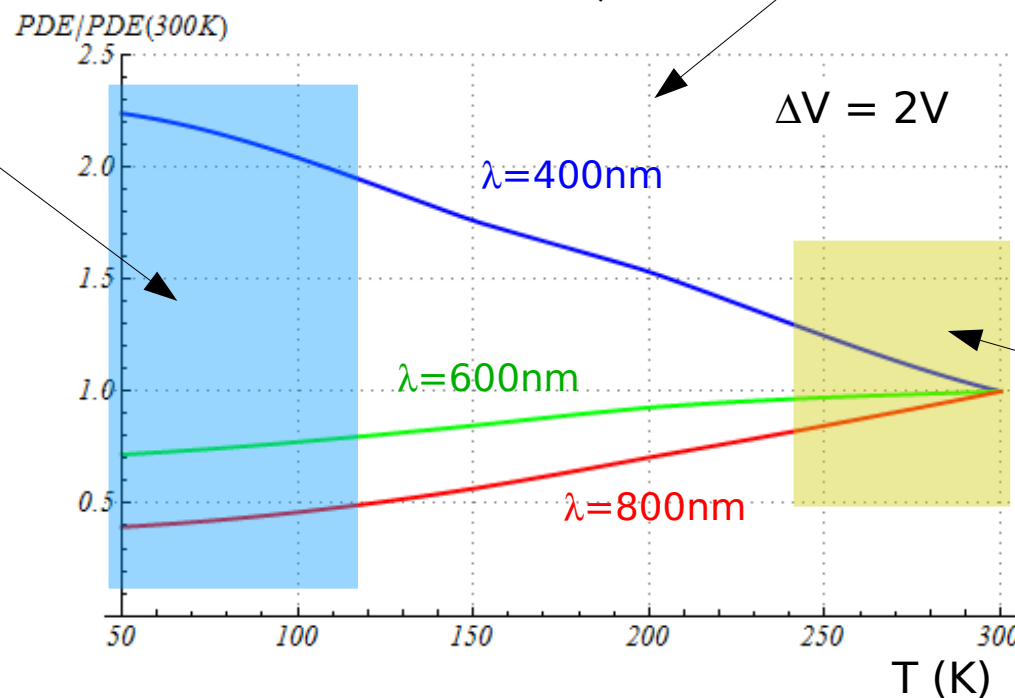


1) main contribution to PDE from electrons
→ PDE distribution shifted toward short λ
at low T because of larger absorption length
(photo-generation deeper into depletion
layer → gain for shorter λ , loss for longer λ)

(see also PDE vs T)

2) tunneling effects not (yet)
included in the model
(enhancement of PDE,
interplay with band gap
variations with T)

3) freeze-out
not (yet)
included in
the model



4) something else
is missing: need
to explain PDE
decreasing with T
for $250K < T < 300K$

to be understood

Conclusions

Basic properties of SiPM (FBK) were measured at low T. Main features are:

- **Breakdown V** decreases non linearly with T, as expected
→ better stability against T variations than at T room
- **Dark rate** reduced by several orders of magnitude
→ tunneling mechanism(s) below ~200K
- **After-pulsing** at % level down to 100K; blow up below 100K
- **PDE** vs T: modulation up to $\pm 50\%$ wrt T room
→ PDE decr. as T 300K \rightarrow 250K, incr. as T 250K \rightarrow 120K, then freeze-out
- **PDE** vs λ : PDE peaks at lower λ as T decreases
- **Cross-talk and Gain** (detector capacity) are independent of T (at fixed ΔV)

Ongoing data analysis ongoing:

- timing resolution vs Temperature (expected to improve at low T)
- after-pulsing characteristic time constant(s) vs T (traps lifetime)
- charge resolution at low T (gain fluctuations)
- cross-check PDE (pulsed vs current method)

Ongoing **modeling** for more detailed understanding of After-Pulsing and PDE features at low T

SiPMs behave very well at low T, even better than at room T

In the range $100\text{K} < T < 200\text{K}$ SiPM perform optimally;

→ excellent alternatives to PMTs in cryogenic applications (eg Noble liquids)



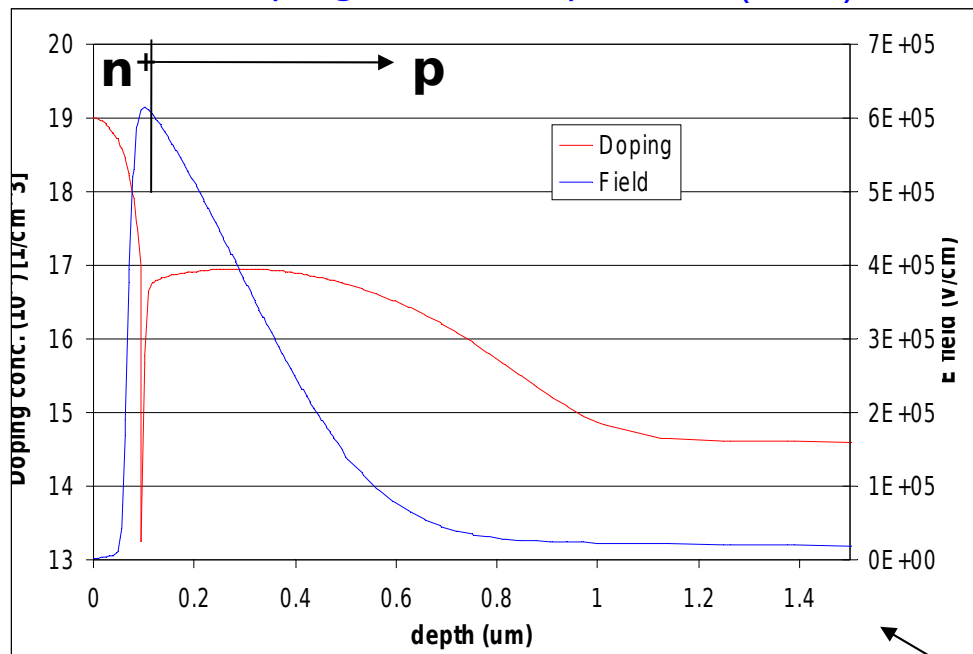
Additional material

G.Collazuol - IPRD10 10/6/2010

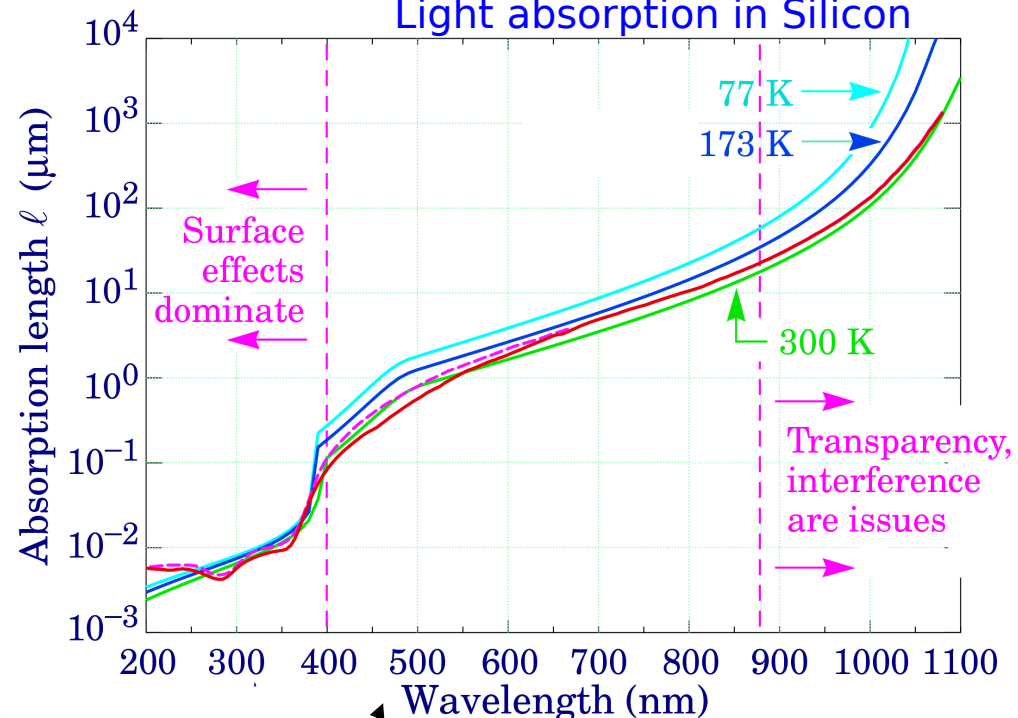


Close up of a cell

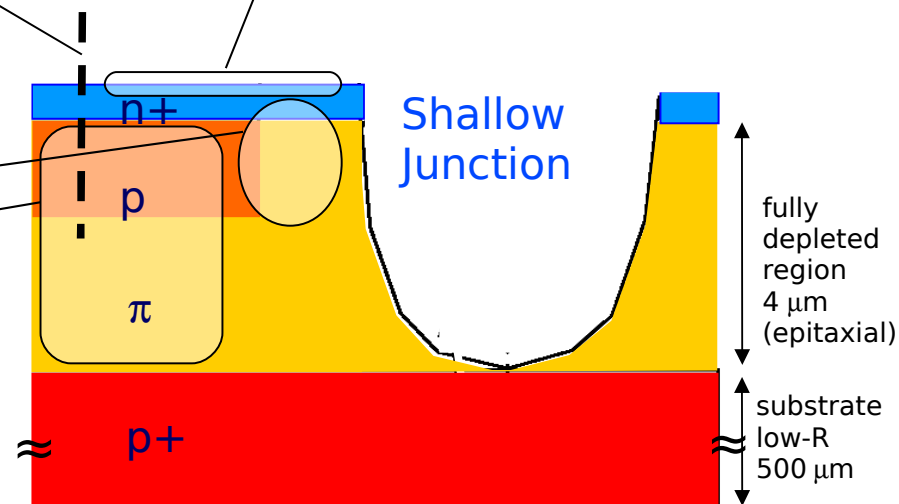
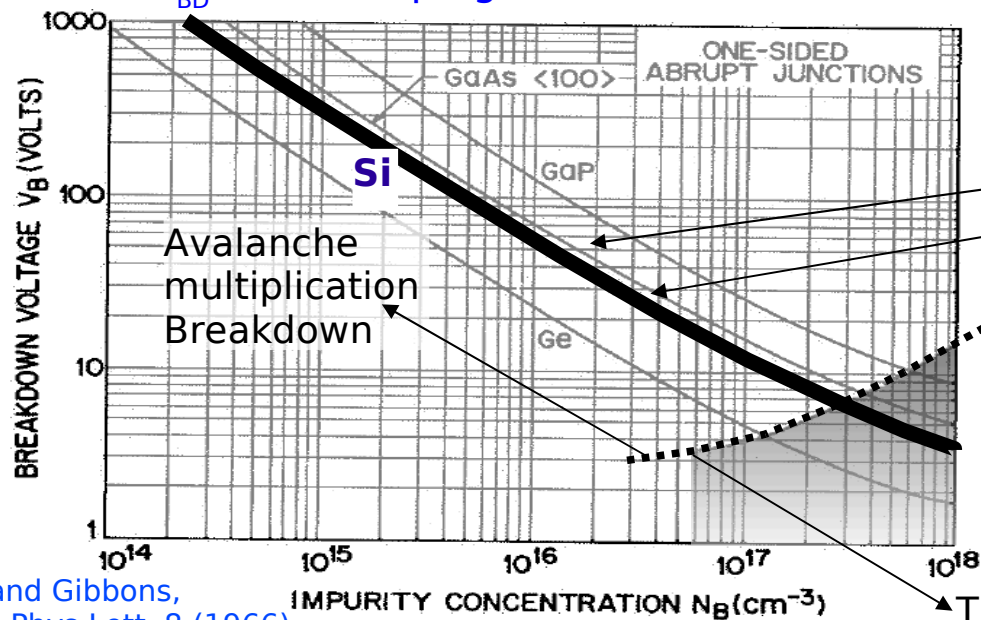
Doping and Field profiles (IRST)



Light absorption in Silicon

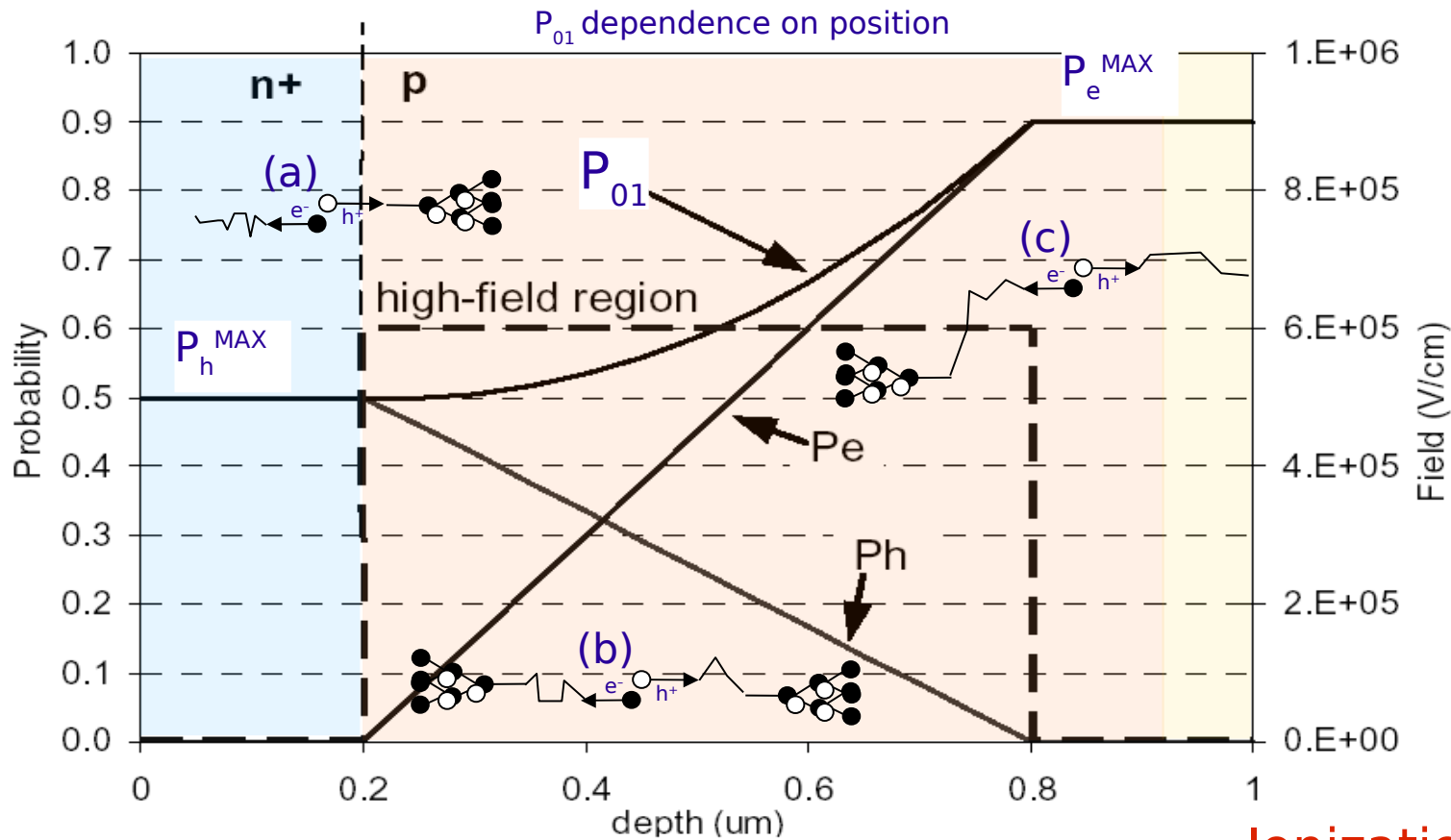


V_{BD} versus doping concentration



Tunneling effect Breakdown

Avalanche trigger probability (P_{01})



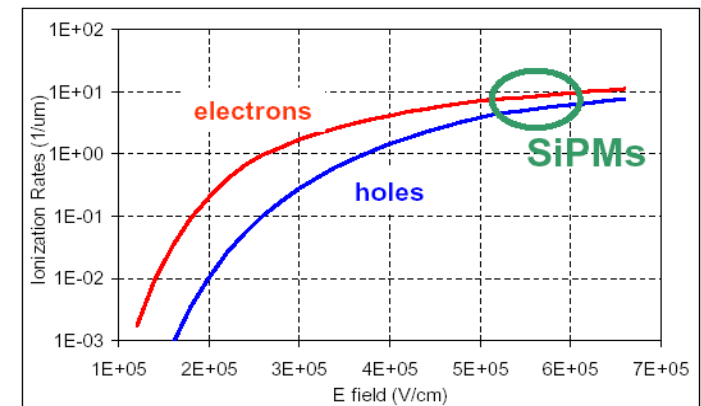
C.Piemonte
NIM A 568
(2006) 224

Example with constant high-field:

- (a) only holes may trigger the avalanche
- (b) both electrons and holes may trigger (but in a fraction of the high-field region)
- (c) only electrons may trigger

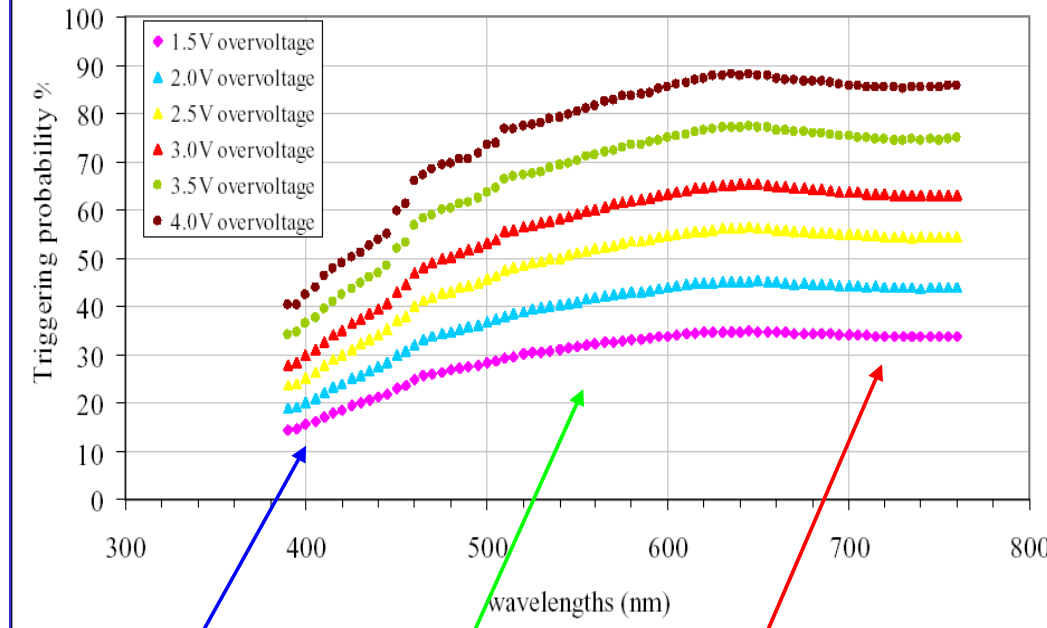
- high over-voltage
 - photo-generation in the p-side of the junction
- P_{01} optimization ←

Ionization rate in Silicon



Avalanche trigger probability (P_{01})

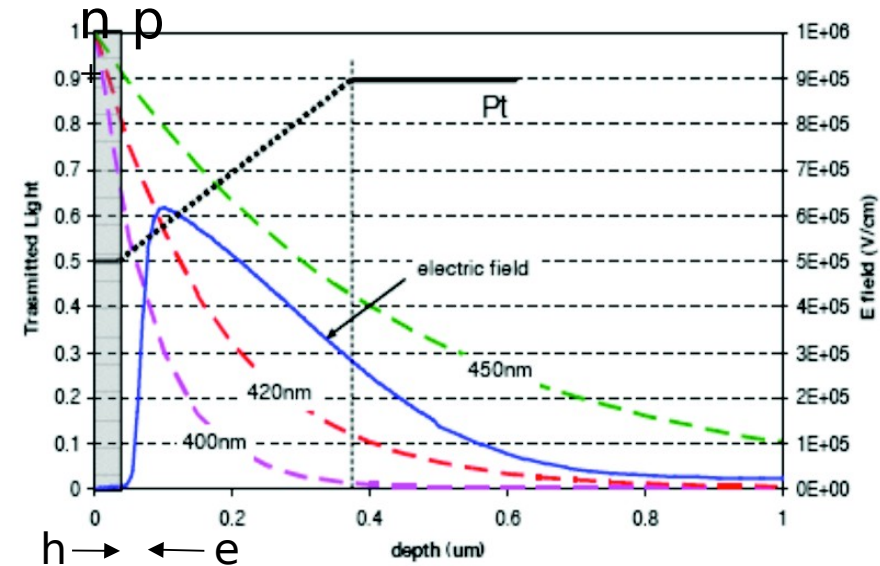
$$P_{01} = \text{PDE} / \text{QE} / \epsilon_{\text{geom.}}$$



Only e^- cross the high E field region and trigger the avalanche

Both h^+ and e^- might trigger the avalanche (but cross only a fraction of high field region)

Only h^+ cross the high E field trigger the avalanche



Silicon properties at low T: higher mobility

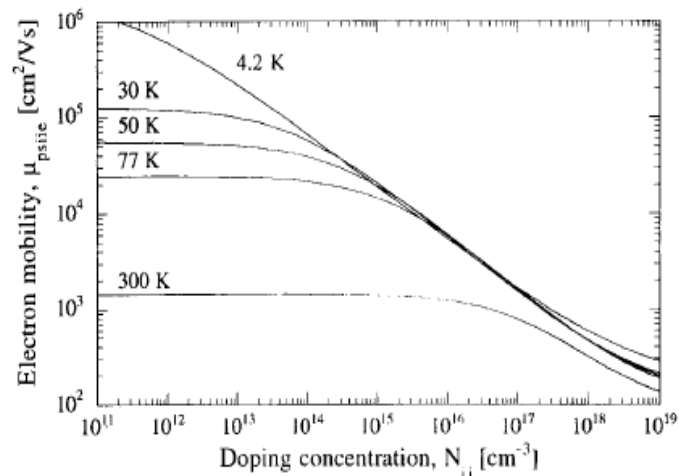


FIGURE 1.16. Calculated electron mobility due to phonon and ionized impurity scattering mechanisms. The five plots correspond to $T = 300, 77, 50, 30$, and 4.2 K.

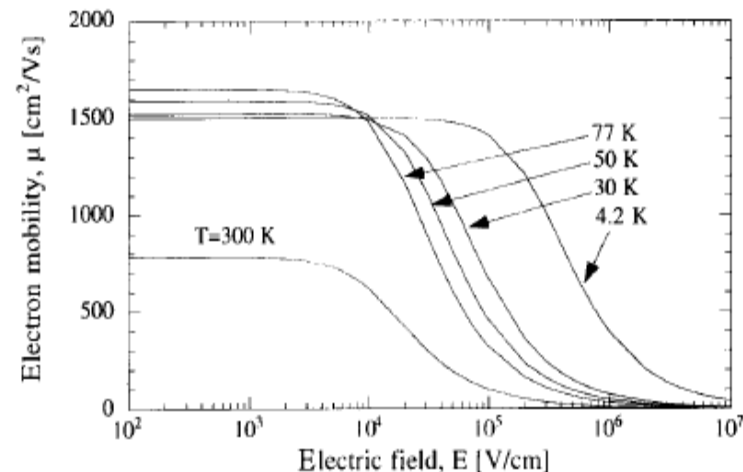


FIGURE 1.17. Calculated electron mobility, due to phonon, ionized impurities, and velocity saturation effects, as a function of the electric field for five temperatures; $N_{ii} = 10^{17} \text{ cm}^{-3}$.

Silicon prop't's at low T: carriers freeze-out

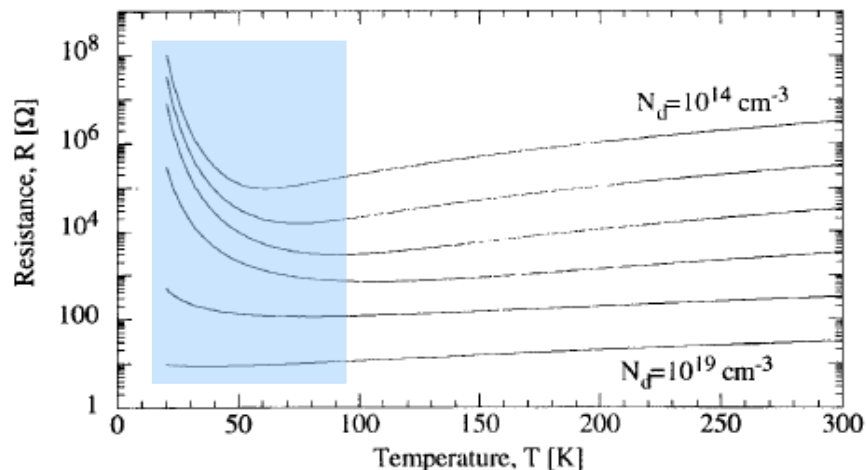


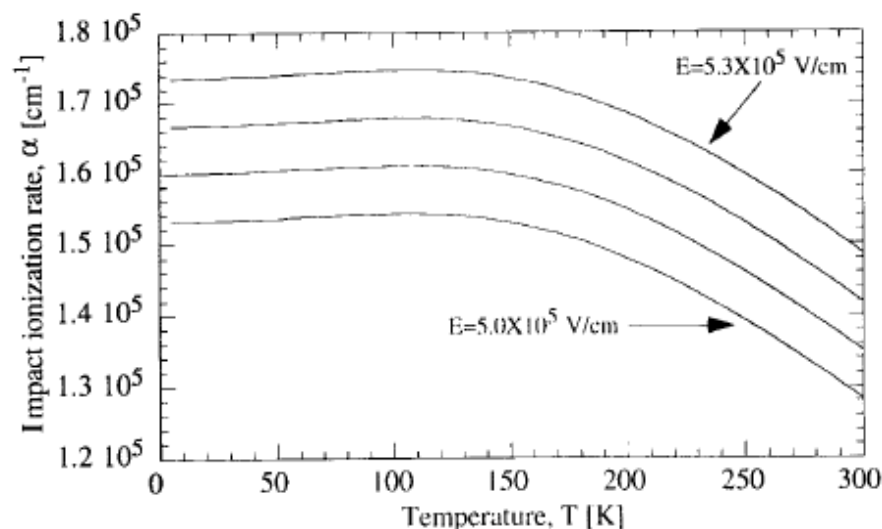
FIGURE 1.14. Calculated electrical resistance of a silicon slab of $(W/L) = 20/50 \text{ μm}$ and depth of 1 μm for different doping concentration levels.

For $T < 100$ K, the ionized impurities act as shallow traps (provided the impurity doping concentration below of $10^{18} \text{ atoms/cm}^2$) and carriers begin to occupy these shallow levels.

For $T < 30$ K, practically no carriers remain in the bands

Plots from Guterrez, Dean, Claeys - "Low Temperature Electronics: Physics, Devices, Circuits and Applications", Academic Press 2001

Silicon propt's at low T: impact ionization



For $T < 77\text{K}$ no data are available \rightarrow modeling is quite difficult...

FIGURE 1.43. The impact ionization rate α as a function of temperature T_A with the electric field E as a parameter calculated from Okuto and Crowell's (85) model.

Silicon propt's at low T: absorption length

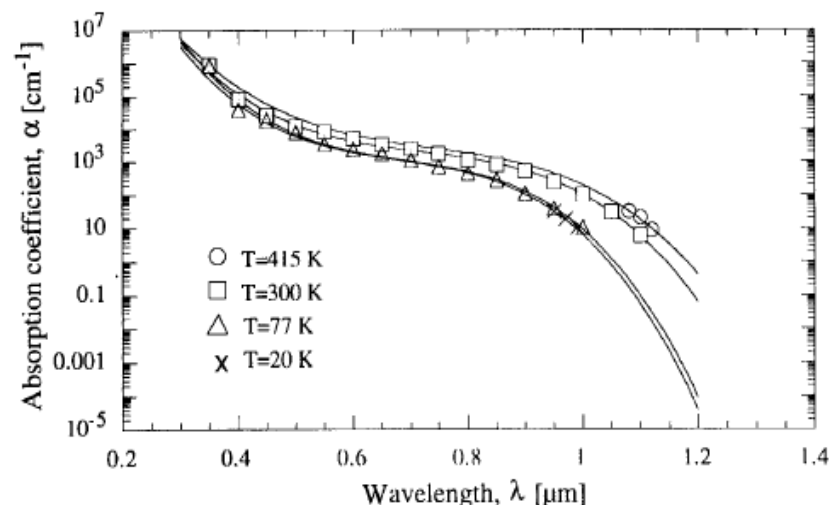


FIGURE 1.53. Experimental (symbols) and fitted (lines) absorption coefficient α of silicon at $T = 415, 300, 77,$ and 20 K [replotted from Rajkanan *et al.* (109)].

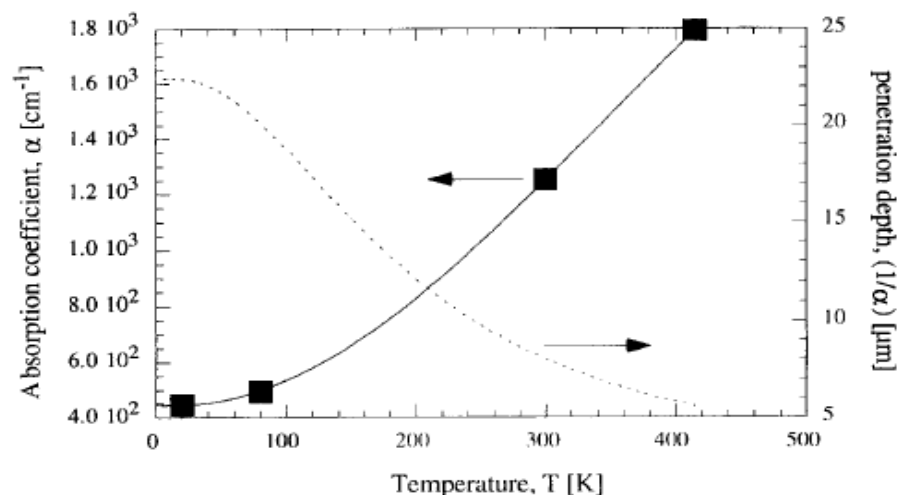


FIGURE 1.54. Measured absorption coefficient α (■) (101) and fitted α (solid line) versus temperature T . On the right axis the fitted penetration depth ($1/\alpha$) is also shown.

Avalanche breakdown vs T

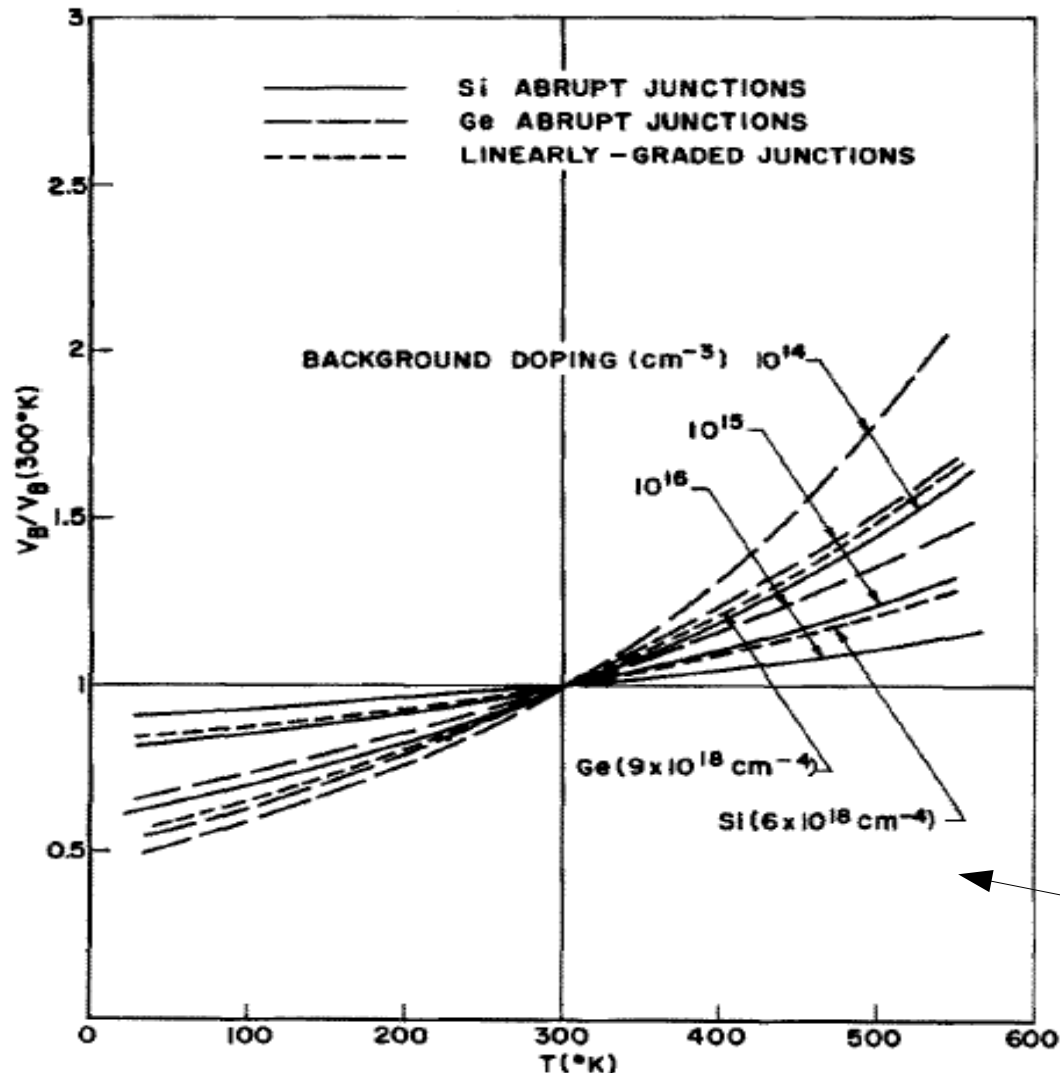


Fig. 4. Breakdown voltage vs temperature for Si and Ge p - n junctions. $V_B(300^\circ\text{K})$ is 2000, 330, and 60 V for Si and 950, 150, and 25 V for Ge for dopings of 10^{14} , 10^{15} , and 10^{16} cm^{-3} respectively. The linear-graded junctions have $V_B(300^\circ\text{K})$ the same as those for doping of 10^{15} cm^{-3} .

Avalanche breakdown V is expected to show a **non linear dependence on T** (depending of the junction type and doping concentration)

Breakdown V decreasing with T due to increasing mobility

NOTE: in freeze-out regime Zener (tunnel) breakdown could be relevant.
→ negative Temperature coefficient (increasing with decreasing T)

Crowell and Sze

More recent model by Crowell and Okuto after Shockley, Wolff, Baraff, Sze and Ridley.

p-n junction characteristics: forward bias

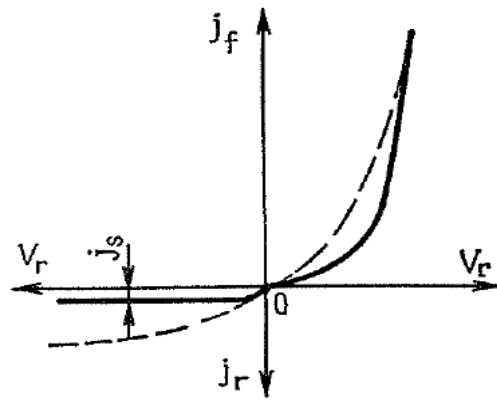
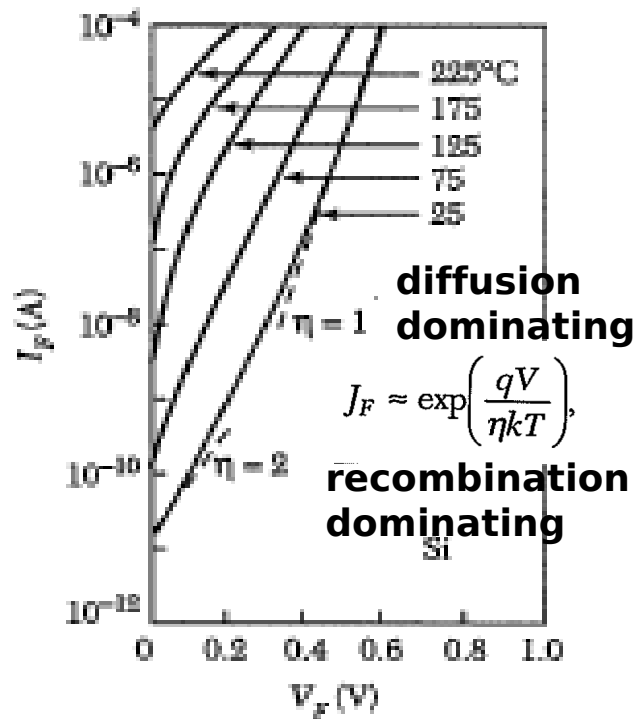
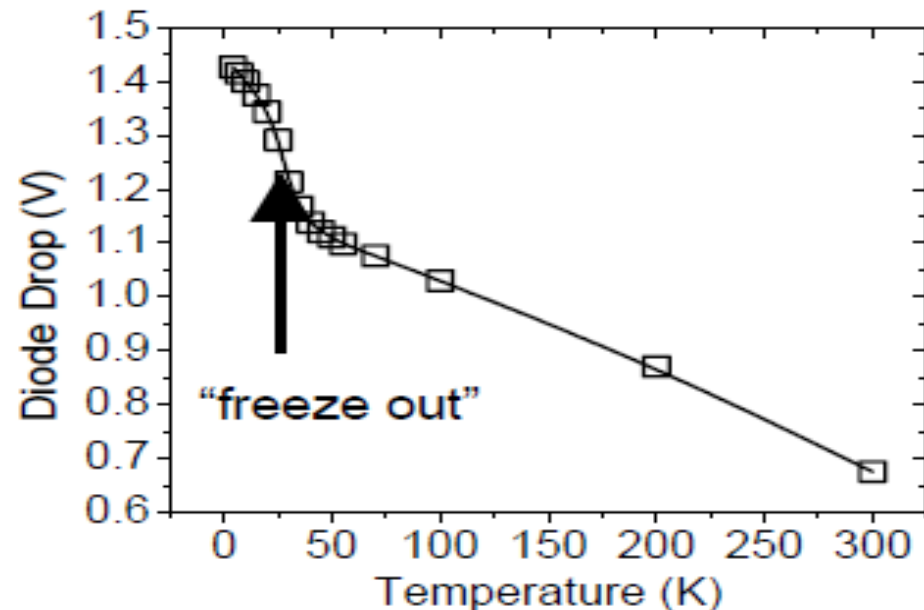
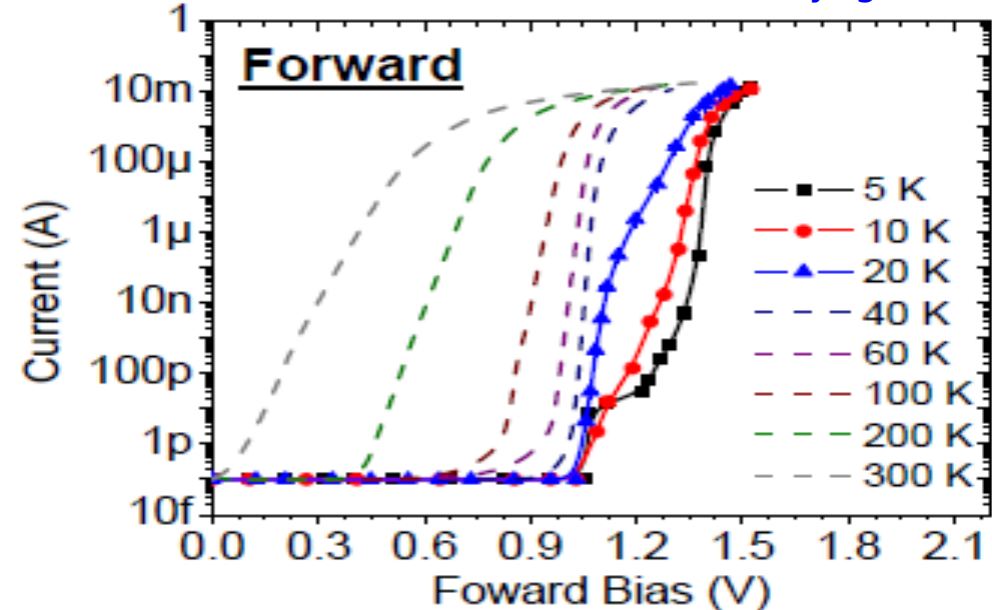


Fig. 8.16. The current-voltage characteristic of a *pn* junction



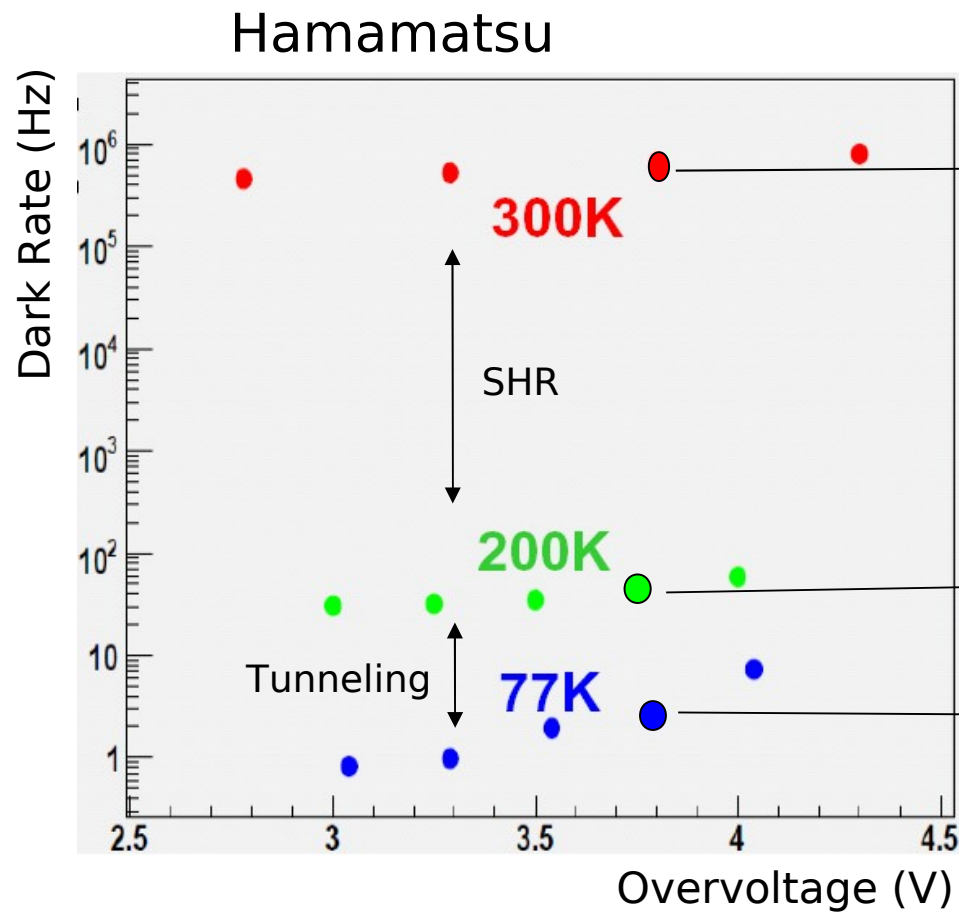
E.Johnson (RMD) at IEEE 2009

“Characterization of CMOS APD at cryogenic T”

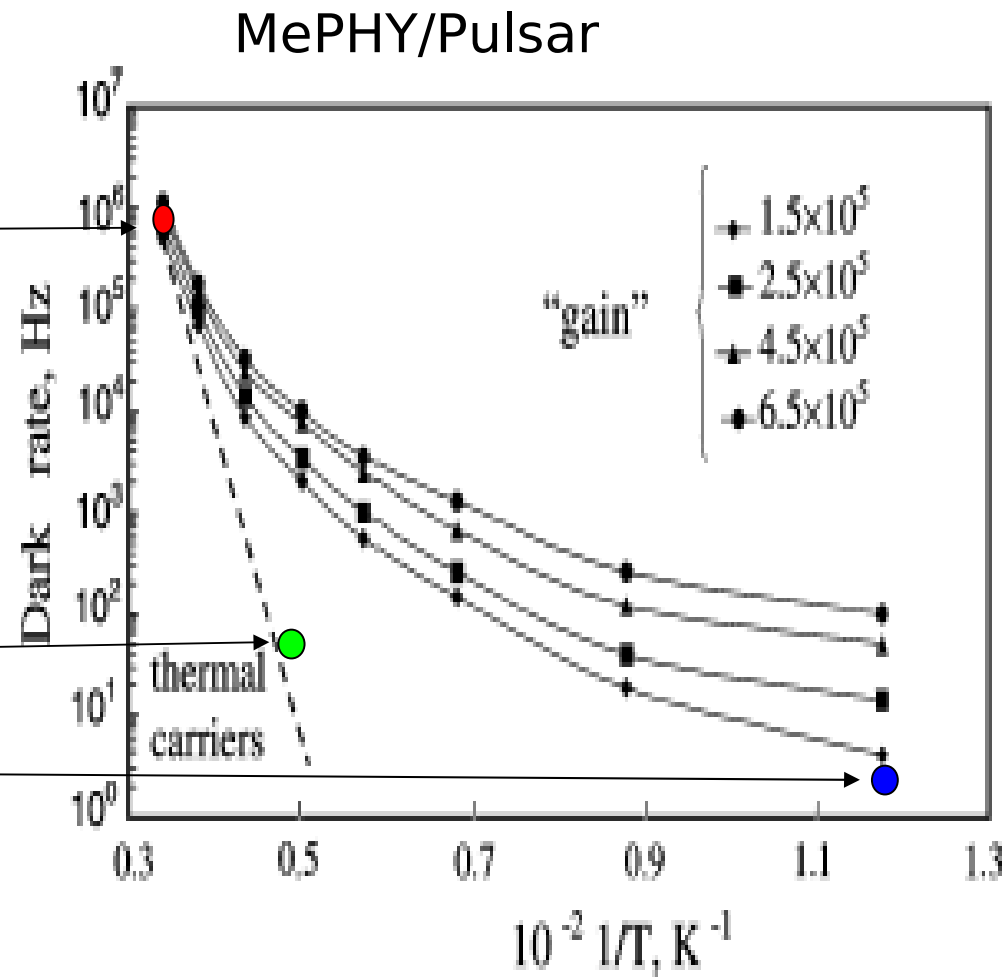


Size - “Semiconductor devices”

Dark Rate



H.Otono - PD07



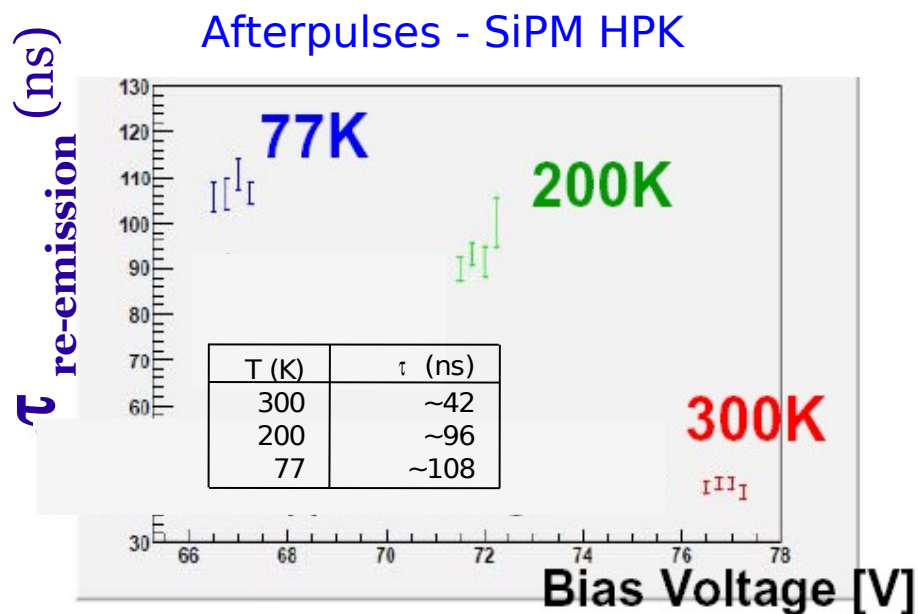
Dolgoshein et al, NIM A 442 (2000)

Electric field engineering and silicon quality
make huge differences in dark noise as a function of T

T dependence: after-pulse, cross-talk

After-pulses: increases at low T

Trap lifetime decreases as T increases

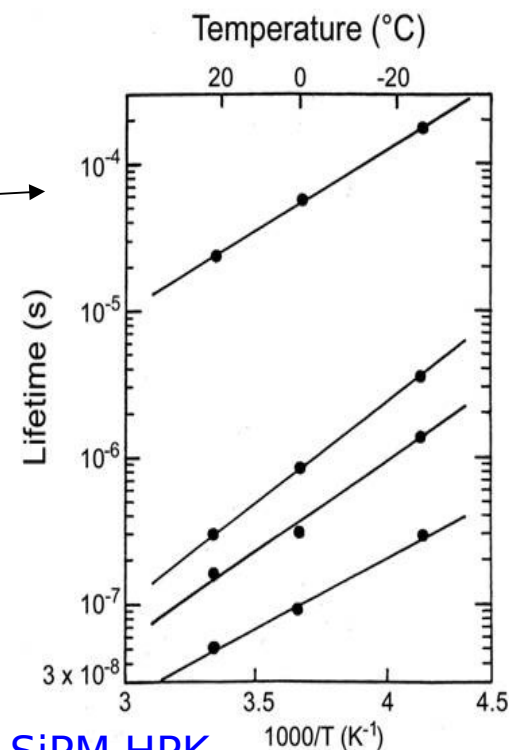
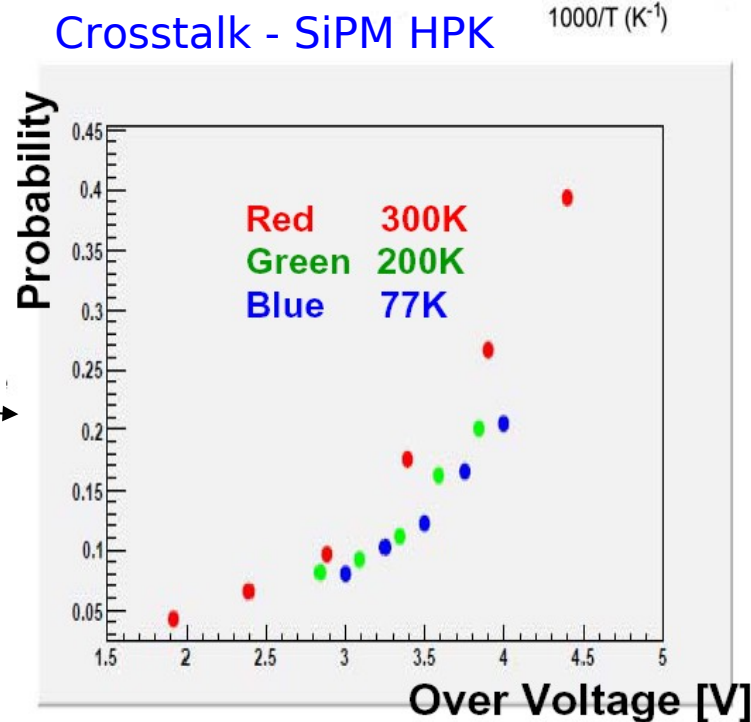


H.Otono - PD07

Cross-talk: decreases at low T

Observed slight reduction at low T

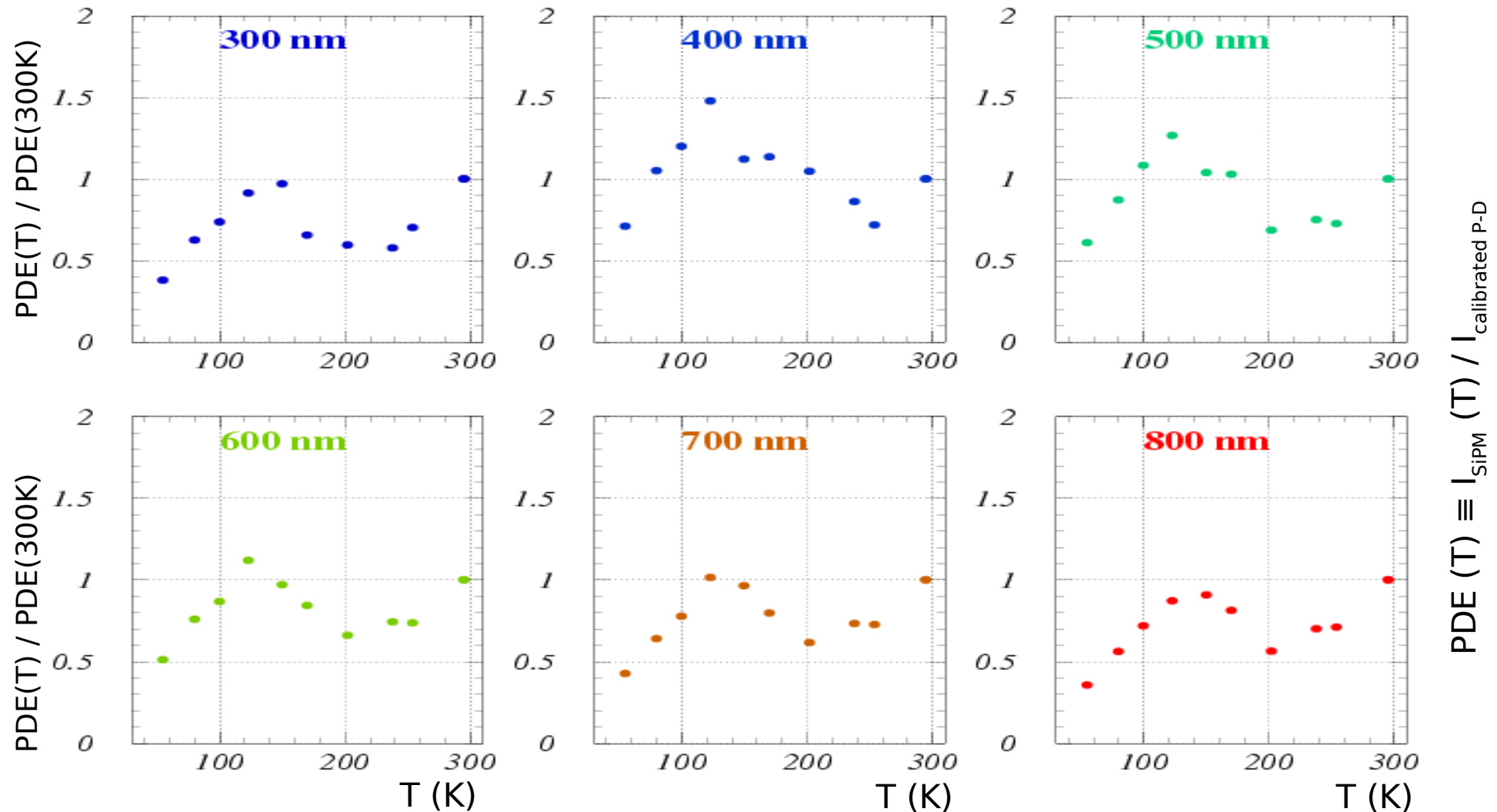
(I guess: due to lower PDE for long wavelength photons which dominate the carrier luminescence spectrum)



S.Cova, A.Lacaita,
G.Ripamonti, IEEE EDL (1991)

PDE at various λ – T scan ($\Delta V = 2V$)

PDE dependence on T at fixed gain. Normalization with calibrated photo-diode current and with PDE at T=300K (double ratio)

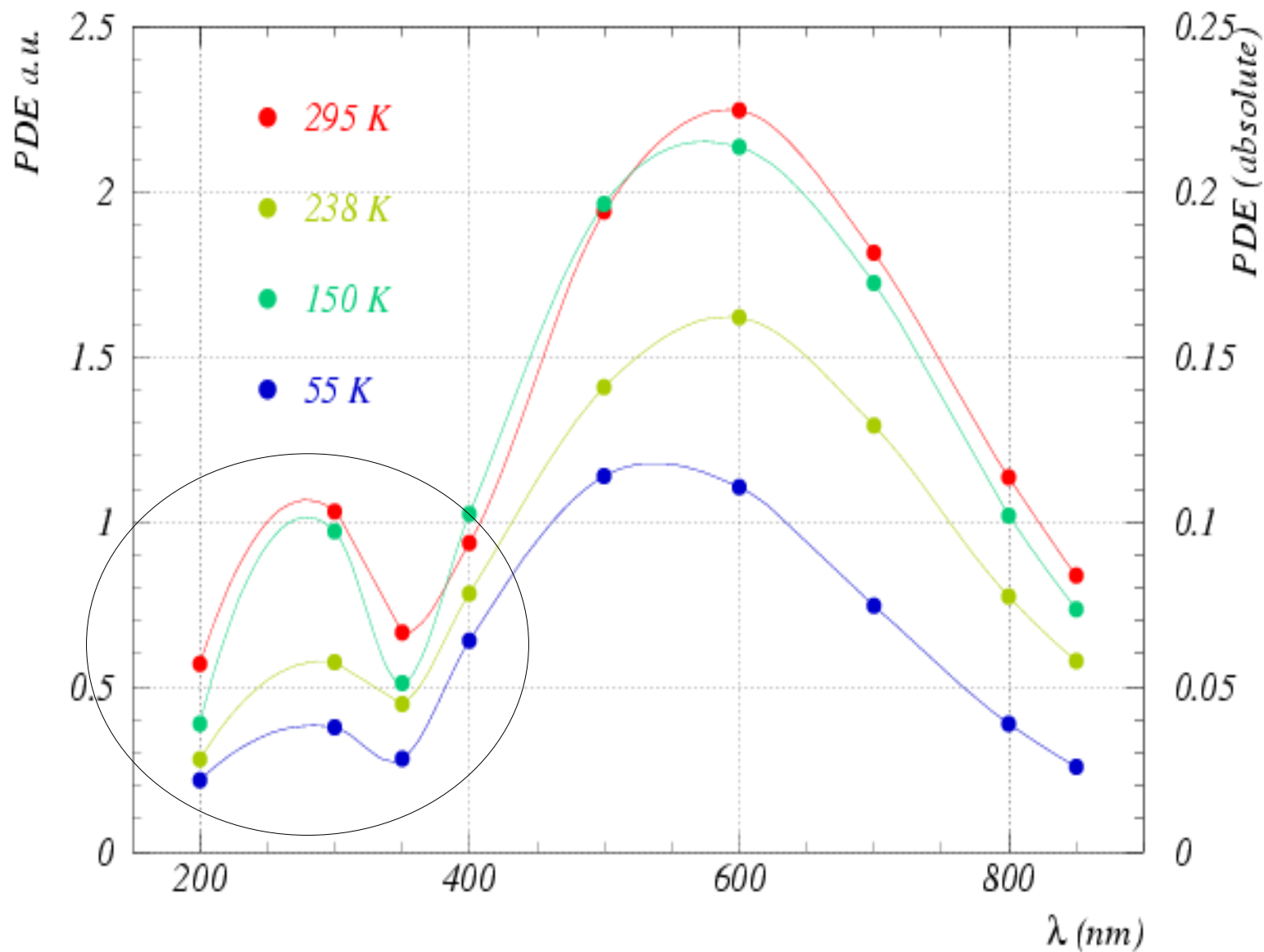


$$\text{PDE}(T) \equiv I_{\text{SiPM}}(T) / I_{\text{calibrated P-D}}$$

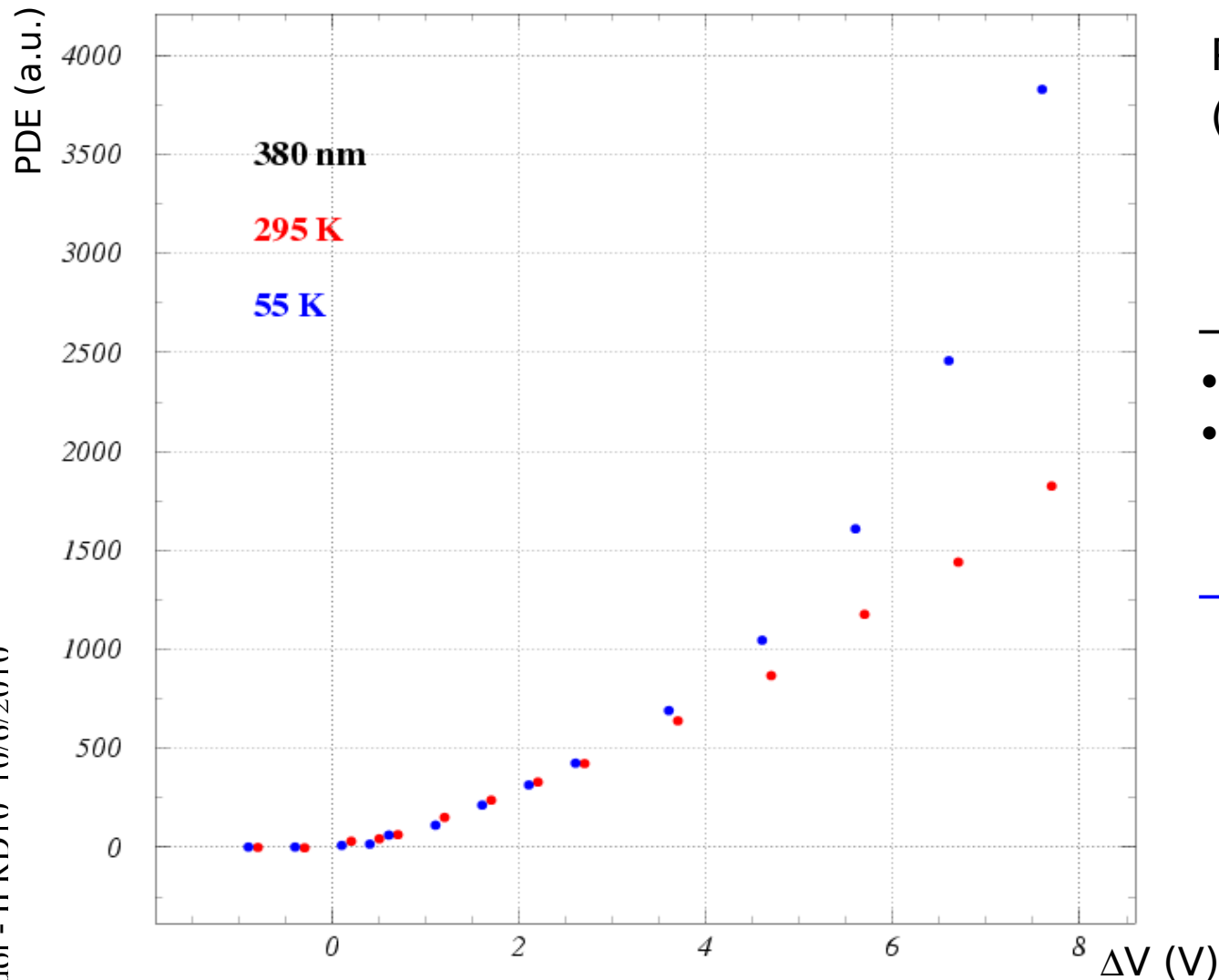
- **shape** similar at different $\lambda \rightarrow$ **related to properties of multiplication /recombination**
- lower efficiency at low T for longer $\lambda \rightarrow$ **due to absorption length $\sim 1/T$ (with constant depletion width)**

PDE vs λ (constant $\Delta V=2V$) - halogen lamp (CW)

$$PDE = I_{\text{si pm}} / G / I_{\text{photons}}$$



PDE vs ΔV (constant T) with LED (380nm)



$$\text{PDE (a.u.)} \equiv I_{\text{SiPM}} / I_{\text{LED}} / \Delta V$$

(Dark rate subtracted)

→ At higher ΔV :

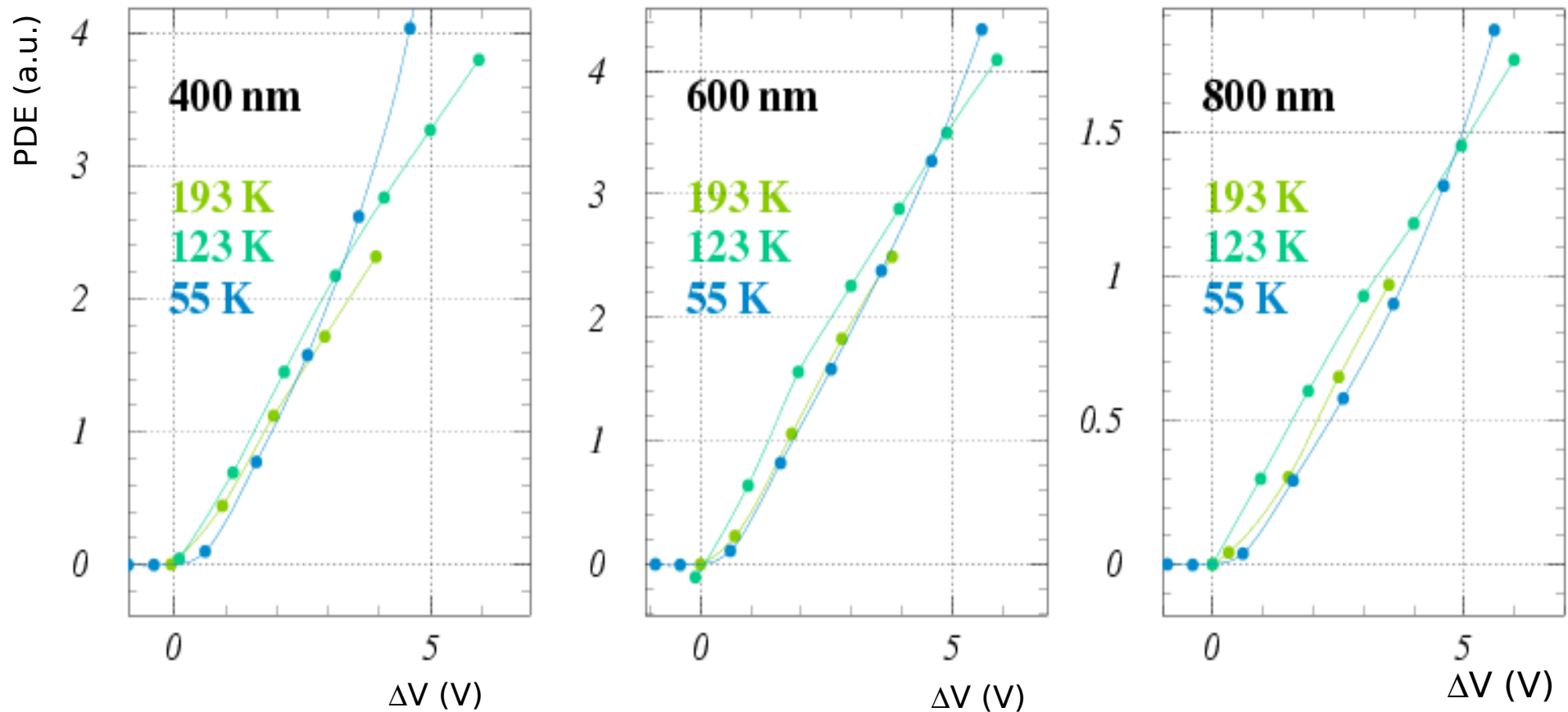
- 55K affected by After-Pulses
- 295K less affected by AP

→ Slope PDE/ ΔV (at small ΔV)
independent of T

PDE vs ΔV (constant T) - λ scan - halogen lamp (CW)

PDE vs ΔV measured as Current/Gain \rightarrow PDE (a.u.) $\equiv I_{\text{SiPM}} / I_{\text{calib}} / \Delta V$

Normalization to calibrated photo-diode current (not absolute # of photons)



- 193K and 123K measurements not affected by after-pulses \rightarrow saturation visible
- 55K affected by after-pulses (not corrected; cross-talk is not subtracted too)

(Dark rate subtracted - small effect)

PDE (SPAD/APD devices)

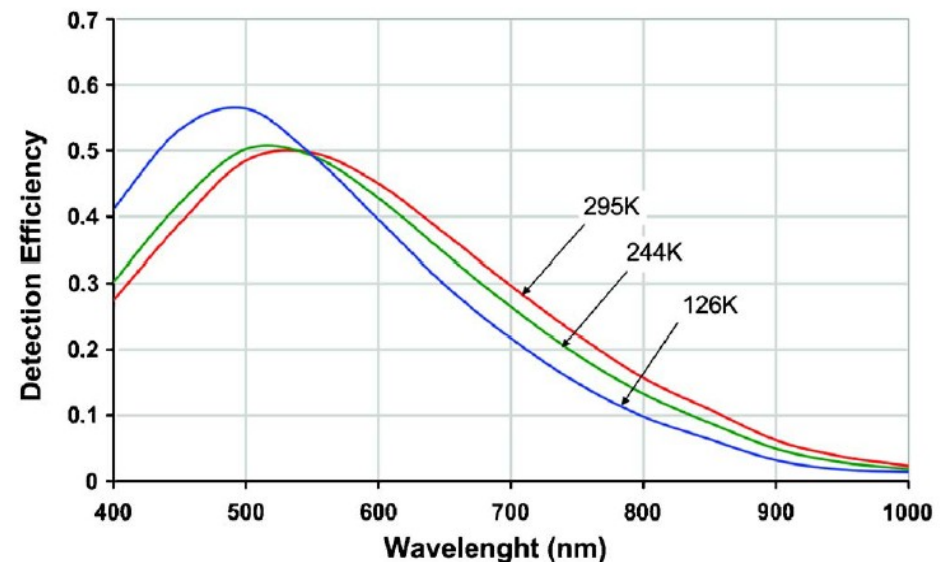
PDE dependence on T (Over-voltage fixed)

Combination of various effects:

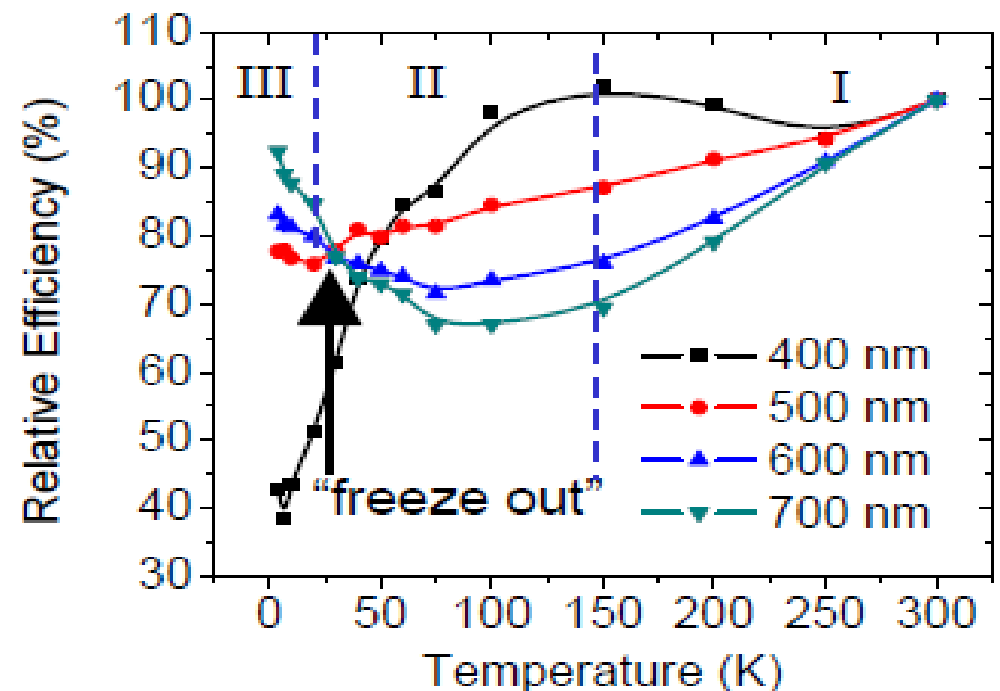
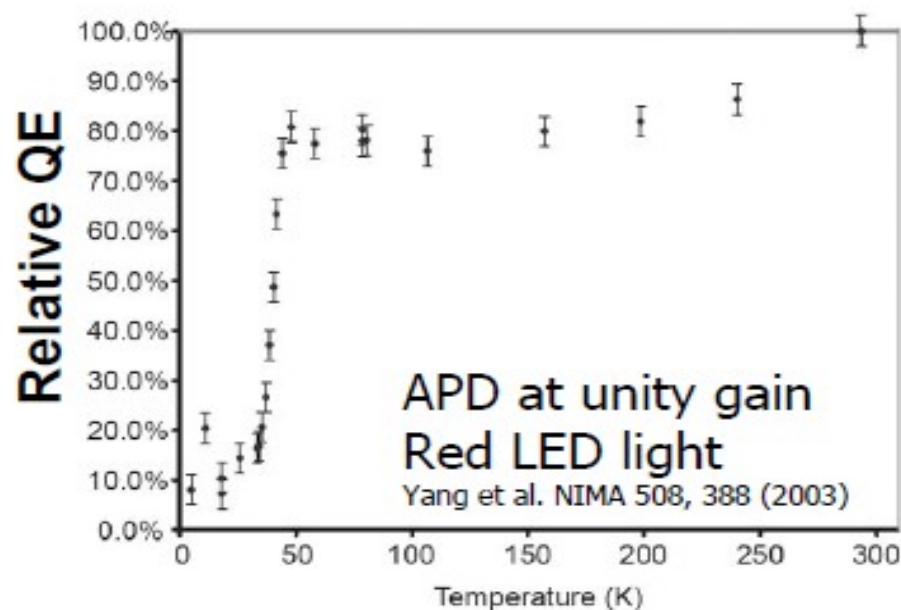
- P_{01} increases at low T because of increased impact ionization
- Optical attenuation length increased (Energy gap increases) at low T
- Depletion region widening in APDs, but not in SiPM which are fully depleted

Similar effect expected also for SiPM

SPAD: Cova et al, Rev.Sci.Instr. 7 (2007)



APD: Johnson et al (RMD) IEEE 2009

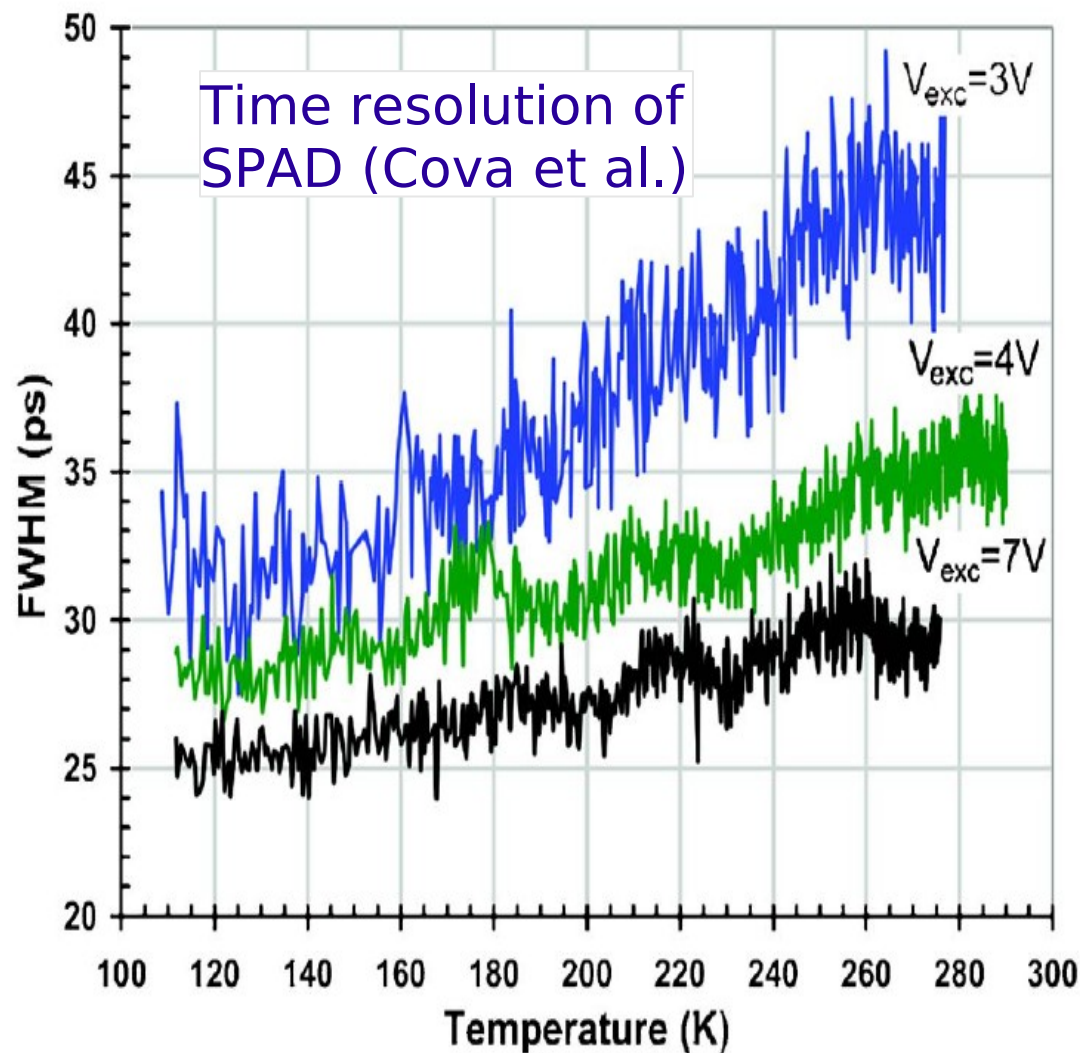


Timing (SPAD devices)

Timing: better at low T

Lower jitter at low T due to higher mobility

(Over-voltage fixed)



I.Rech et al, Rev.Sci.Instr. 78 (2007)